TRANSVERSE RELAXATION TIMES OF MAJOR BRAIN METABOLITES

IN GULF WAR ILLNESS

APPROVED BY SUPERVISORY COMMITTEE

Dr. Richard Briggs, Ph.D.

Dr. Vikram Kodibagkar, Ph.D.

Dr. Roderick McColl, Ph.D.

Dr. Sergey Cheshkov, Ph.D.

Dr. Changho Choi, Ph.D.

For Nan, who makes everything possible

With infinite patience, tireless support,

And boundless love.

TRANSVERSE RELAXATION TIMES OF MAJOR BRAIN METABOLITES IN GULF WAR ILLNESS

by

AUDREY JENNIFER CHANG

DISSERTATION

Presented to the Faculty of the Graduate School of Biomedical Sciences

The University of Texas Southwestern Medical Center at Dallas

In Partial Fulfillment of the Requirements

For the Degree of

DOCTOR OF PHILOSOPHY

The University of Texas Southwestern Medical Center at Dallas

Dallas, Texas

April, 2010

ACKNOWLEDGEMENTS

It may be a common perception that the academic journey is a lonesome one. I developed this view myself, watching loved ones before me and colleagues around me prepare dissertations in a vacuum of solitude, alone with nothing but papers and textbooks for companionship. But in a moment of reflection and introspection, I find that initial assumption to be false. For I didn't arrive at this place in my journey alone, and I have not made a single stride forward that has not been both inspired by, and immeasurably improved by the generous support and guidance of those around me.

I'd like to thank first Richard Briggs, Ph. D., for the obvious: for giving me a fantastic opportunity, for instigating and motivating my research, for keeping me informed and keeping me focused, and of course, for his invaluable insight and knowledge of the field. I'd also like to thank him for the less obvious: for teaching me independence, for teaching me critical assessment, for being the representation of integrity, fairness, and diligence in all things, research and otherwise.

I'd like to recognize Sergey Cheshkov, Ph. D., for he is never recognized enough in my day to day debates with him on the nature of spectroscopy. Whenever I was faced with an obstacle, or worse, a limitless set of confounds, his experience was my compass, and I was able to find a path to follow. He took on the mantle of responsibility for the both of us – no easy task, I'm sure – and always was in my corner, even if everyone else

was against me. That's not something that should be taken lightly, and I will be forever grateful for his support, his patience, and his generosity.

I would also like to thank my committee as a group – Dr. Briggs, Dr. Cheshkov, Dr. Kodibagkar, Dr. McColl, and Dr. Choi. It is a tremendous gift, being able to choose one's committee members – to select five people who you not only admire, but seek to emulate. My committee members are both measuring stick and signposts on a long trek. They not only provide goals for me to aspire to, but guidance and support in turbulent times. I feel that they have gone above and beyond the call of duty on my behalf, and their selflessness in this cannot be overstated.

My work is supported, fully and enthusiastically, not just underwritten, by Dr. Robert Haley, M.D., who is the central source and motivation for not only my research, but many others. But more than that, he has always inspired with his energy and selfless interest for helping others, and his endorsement of my research cannot be given a value. I will forever strive to be as passionate about my work as he has been throughout, in the face of adversity or even apathy.

I'd like to thank Subhendra Sarkar, Ph. D., Evelyn Babcock, Ph. D., and Victoria Webster not only for their assistance at the magnet, but for their uniformly enthusiastic encouragement. They are all three truly excellent role models for professionalism and patient care and have taught me so much just by their consummate example in the lab.

To the other members of my sub-core, Hyeonman Baek and Sandeep Kumar Ganji, a warm thank-you that can only be expressed between members of the same team. We've gone head to head on every issue and been back to back in bad circumstances.

Your support and encouragement has been crucial to my work for as long as you've been a part of our group.

Those outside the scientific community, if I may take an extra moment, have been a bigger part than they will ever know. Even though friends and family cannot give advice or insights into my research or results, they offer unwavering support – a kind of blind faith in abilities and knowledge they have never seen from me – and that is truly inspiring. To know that there are people out there who consider you to be up against insurmountable odds and already assume you to be the victor, helps to make those odds look less insurmountable, after all.

And finally, I'd like to thank my husband, Han Nan, though words will never contain the kind of thanks he deserves. He not only supported and encouraged me every moment of this journey, he is the reason I am who I am, and of course something like that can never be repaid. Though all of this was brought together and inspired by others, though it was carried out by me, though these pages were written *by* me, it is, and always will be, *for* him.

Transverse Relaxation Times of Major Brain Metabolites in Gulf War Illness

Audrey Chang, Ph.D.

The University of Texas Southwestern Medical Center at Dallas, 2010

Mentor: Dr. Richard Briggs, Ph.D.

Because many neurodegenerative diseases, like Gulf War Illness (GWI), are unidentifiable on conventional MRI or other imaging modalities in their early stages, diagnosis and treatment must wait until the disease has progressed to a more debilitating and obvious phase. The first aim of this thesis was to develop a reliable protocol to investigate the more subtle changes in metabolite concentrations and T_2 relaxation times in GWI. This protocol generated reproducible MRS results, with small inter- and intra-subject variability, on normal controls in the basal ganglia region using single voxel

spectroscopy. The second aim of this thesis was to compare T_2 values of major brain metabolites in the basal ganglia in Gulf War Syndromes 1-3 and age-matched control veterans. Significant differences were found between Syndrome 2 and controls for NAA and Cr in left basal ganglia and for Cho in right basal ganglia. Finally, measured T_2 values were also used to correct concentrations of brain metabolites to investigate relaxation effects on concentration results. At low TE values (TE=30 ms in this study) T_2 relaxation measurements were found to have a small effect (approximately 10%) on concentration data. At larger TE values (TE=270 ms in this study) T_2 relaxation measurements have a greater impact on concentration results. This finding reinforces the concentration data as evidence of neurophysical damage underlying cognitive difficulties experienced by Gulf War Illness patients, instead of T_2 time effects creating false differences in concentration or metabolite signal ratios.

By establishing a dependable and efficient method of acquisition, T_2 relaxation measurements can be incorporated into future MRS protocols, ensuring metabolite concentration measurements can be accurately corrected, especially for acquisitions with long TE, instead of using a static quantity, and moving the analysis of single voxel spectroscopy towards true absolute quantitation values. Also, this method, confirmed here to be reliable on existing equipment, can be expanded for use in other disease models which are similarly difficult to detect in conventional MRI.

TABLE OF CONTENTS

LIST OF FIGURES

LIST OF TABLES

LIST OF ABBREVIATIONS

SPECTROSCOPY:

MRI – Magnetic Resonance Imaging

fMRI – Functional Magnetic Resonance Imaging

SVS – Single Voxel Spectroscopy

PRESS – *P*oint *R*esolved *S*pectroscopy

STEAM – Stimulated Echo Acquisition Mode

NAA – N-Acetylaspartate

Cr_t – Creatine (total of phosphocreatine and creatine)

Cho_t – Choline (total choline, phosphocholine, and glycerophosphocholine)

PROFILING:

GWI – Gulf War Illness

PTSD – Post-Traumatic Stress Disorder

OPIDP – Organophosphate-Induced Delayed Polyneuropathy (OPIDP)

RNMCB-24 – Twenty-fourth Reserve Naval Mobile Construction Battalion

CB – Construction Battalion

DEET – Di-Ethyl-Toluamide

PAI – Personality Assessment Inventory

NEUROANATOMY:

LBG – Left Basal Ganglia

RBG – Right Basal Ganglia

1 BACKGROUND AND INTRODUCTION

The aim of this study is to measure transverse relaxation times (T_2) *in vivo* of major brain metabolites (NAA, Cr_t, and Cho_t) in specific brain areas of Gulf War Illness (GWI) patients as compared to normal controls. The determination of this potentially changing factor can affect and inform concentration data results, giving insight on the true nature of previously established significant concentration differences between ill Gulf War veterans and normal control metabolite data, as well as moving our data acquisition and analysis one step closer to true absolute quantitation of metabolite concentrations in the human brain.

In order to achieve this aim, it is first necessary to establish a reproducible and sensitive technique for measuring the potential T_2 relaxation time changes in GWI and similar neurodegenerative disease patients, while keeping within appropriate scanner time limits.

1.1 Gulf War Illness

1.1.1 Brief History of the Persian Gulf War and Gulf War Illness

The Persian Gulf War occurred in the late part of 1990 and the early months of 1991, after Kuwait was invaded by Iraq on August 2, 1990. The United States immediately responded with Operation Desert Shield, designed to be a defensive mission to protect Saudi Arabia from invasion by Iraq. By January 15, 1991, the United Nations authorized military action to oust Iraqi soldiers from occupation of Kuwait, and soldiers from a coalition of 34 nations deployed to the region, though the majority of forces came from the United States, Saudi Arabia, the United Kingdom, and Egypt.

While overall losses were unexpectedly minimal – reportedly only 113 of the nearly 700,000 US troops were lost to enemy fire – the real controversy began after armed forces returned from the theatre. As of the year 2000, 183,000 military personnel sent to the Gulf War have been declared permanently disabled, and 30% have registered in a database of veterans afflicted with Gulf War Illness (GWI).

Though there were conflicting scientific reports about the existence and nature of Gulf War Illness, on November 17, 2008, the Congress-appointed Research Advisory Committee on Gulf War concluded that “scientific evidence leaves no question that Gulf War illness is a real condition with real causes and serious consequences for affected veterans.”(United States. Dept. of Veterans Affairs. Research Advisory Committee on Gulf War Veterans' Illnesses. 2008).

The estimated incidence of Gulf War Illness, as recognized by the Department of Defense and the Veteran's Association, is approximately 1 in 4 of the almost 700,000 Gulf War veterans. Symptoms of GWI include chronic fatigue, headaches, loss of balance, memory problems, joint and muscle pain, and general indigestion (Kang, Li et al. 2009). Several other symptoms that have been investigated as being potentially linked to GWI are numbness, loss of muscle, bowel, or bladder control, problems with sexual function or fertility, problems with sleep, problems with attention or concentration, swollen glands, fever or night sweats, hair loss, rashes, changes in emotional state, unexplained muscle pain and weakness, and rashes (Haley, Kurt et al. 1997). Other issues potentially related to service during the Gulf War include birth defects, brain cancer, fibromyalgia, and amyotrophic lateral sclerosis (Haley 2003).

These myriad and non-uniform symptoms create a difficulty in diagnosis and evaluation of GWI. Not all the veterans who claim to have GWI have the same set of symptoms, thus creating the need for syndrome classification and segregation. Additionally, the rapidly aging population creates another confound: other diagnosed conditions and the natural progression of aging causing problematic symptomology. These issues are further complicated by the fact that symptoms of GWI could never be correlated with visible changes in magnetic resonance images (MRI) (Haley, Hom et al. 1997), nor with any increase in hospitalization or death rate (Knoke and Gray 1998). Additionally, the source of GWI has not been clearly identified, though it is thought to be related to exposure to neurotoxic chemicals, including organophosphate pesticides and nerve agents (Haley and Kurt 1997; Haley, Kurt et al. 1997; Hom, Haley et al. 1997;

Haley, Billecke et al. 1999; United States. Dept. of Veterans Affairs. Research Advisory Committee on Gulf War Veterans' Illnesses. 2008).

1.1.2 GWI Research Summary

A study performed by Haley, Kurt, and Horn analyzed the self-reported symptoms of 249 members of the Twenty-fourth Reserve Naval Mobile Construction Battalion (RNMCB-24) to objectively determine the presence of a coherent syndrome or illness (Haley, Kurt et al. 1997). The survey was designed after reviewing the reports of approximately 2000 ill veterans as well as reports concerning potential environmental exposure. Both ill and well veterans were asked to participate, as well as active and retired members of the RNMCB-24. Only 30% of the respondents reported good health, and the remaining 70% had a variety of symptoms suspected to be related to wartime exposures. Using two-stage factor analysis, Haley et al. determined 6 orthogonal factors that explained 71% of the total variance in the 52 investigated symptoms scaled in the survey. They described these as discrete syndromes of GWI, and speculated that these multiple factors may be the cause of misdiagnosis of GWI as a variety of other health concerns, such as Post-Traumatic Stress Disorder (PTSD) and chronic fatigue.

- Syndrome 1 was named "impaired cognition" due to common symptoms of attention, and short- and long-term memory problems, difficulty with thinking and reasoning, fatigue and sleep disorders, headaches, and balance/coordination problems.

- Syndrome 2 was named "confusion-ataxia" for problems rooted in thinking and reasoning, confusion, depression or PTSD, problems with balance and coordination, liver disease, memory problems, and sexual impotence.

- Syndrome 3 was named the "arthro-myo-neuropathy" syndrome because of common muscle pain and weakness, joint pains, numbness of the extremities, fatigue, myalgias, and difficulty lifting heavy objects.

- Syndrome 4 was named "phobia-apraxia" due to episodes of numbness and dizziness in subjects, as well as claustrophobia, nausea, and lack of muscle control.

- Syndrome 5 was named "fever-adenopathy" for the common symptoms of night sweats and swollen glands.

- Syndrome 6 was named "weakness-incontinence" because subjects had bowel and bladder incontinence, as well as numbness in the face (but not the extremities).

These six defined syndromes were also listed against the Personality Assessment Inventory (PAI) (Morey 2007) scores; none of the PAI profiles were representative of PTSD or other known pathologies. Haley et al. considered the first three syndromes (1-3)

to be primary, while the latter three (4-6) exhibited overlapping symptoms from syndromes 2 and 3. [Two other case definitions for Gulf War Illness have been reported, the Steele, or Kansas, definition (Steele 2000), and the Fukuda definition (Fukuda, Nisenbaum et al. 1998).]

In a subsequent study, Haley and Kurt investigated in-depth the case histories and risk factors associated with specific wartime chemical, neurotoxin, and pesticide exposures (Haley and Kurt 1997) in their proposed syndrome categories. The results were strong correlations between self-reported exposure risks and syndromes, further supporting the conclusion that separate syndromes exist, each with separate causes and neurophysical damage profiles. Syndrome 1 was strongly associated with wearing pet flea collars which contained neurotoxic pesticides such as diethyltoluamide, or DEET. Syndrome 2 was strongly associated with ambient exposure to sarin gas, assessed by cross-referencing documented sarin gas munitions detonation (such as the one in Kamisayah) with weather records and maps of troop deployment (including the self-reported location of the individual). Syndrome 3 was strongly associated with wearing high concentrations of diethyltoluamide (DEET) insect repellants. Syndromes 2 and 3 also correlate with self-reporting adverse reactions to the prophylactic pyridostigmine bromide tablets given to soldiers prior to deployment to protect against nerve gas exposure.

In these neurological studies of Gulf War veterans (Haley, Hom et al. 1997; Hom, Haley et al. 1997), prior studies (Savage, Keefe et al. 1988; Jamal 1995) on organophosphate and other cholinesterase-inhibiting chemicals in which subjects

exhibited similar symptom profiles were referenced. Following their hypothesis that the various syndromes of GWI were each caused by wartime exposures to organophosphates and/or cholinesterase-inhibiting compounds, Hom et al. compared GWI symptoms to studies in organophosphate-induced delayed polyneuropathy (OPIDP). The similarities included deficits in motor and cognitive skills, and significantly poorer performance in neuropsychological measures such as the Average Impairment Rating, VIQ, and FSIQ as compared to age-matched normal controls. Additionally, OPIDP subjects have a similar absence of abnormalities in conventional imaging and EEG exams. Later government reports and other inquiries into the presence of neurotoxic chemicals in the field also supported this hypothesis (National Institutes of Health (U.S.). Office of the Director. 1994).

An enzymatic analysis of symptomatic veterans also revealed a lower blood level of paraoxonase-1 (PON1) type Q (PON-Q) arylesterase as compared to matched controls (Haley, Billecke et al. 1999). PON-Q works to hydrolyze organophosphates, and is thought to be a genetic marker for predisposition to adverse symptoms. In a similar study of PON1 in Parkinson's disease, the same genetic lack of PON1 creates a susceptibility to degeneration of basal ganglia and substantia nigra regions of the brain.

1.1.3 Current Gulf War Illness Research Efforts at UT Southwestern

The Gulf War Illness Research group at UT Southwestern, the overarching research collaboration to which this study contributes, began studies of deployed veterans and age-matched (deployed as well as un-deployed) controls in June of 2008, with the

purpose of studying GWI and establishing disease models to better identify and treat afflicted veterans.

This large collaborative effort will include research on cerebral blood flow, neuropsychological evaluation, functional magnetic resonance imaging, and electroencephalography, among other studies. However, a central and immediate purpose of the study is to reconfirm findings from the original Haley spectroscopy study (Haley, Marshall et al. 2000) performed in 1998, which clearly demonstrated biochemical and cognitive changes in the affected population, mainly in the basal ganglia and pons regions, but also potentially localized in the hippocampus of ill subjects.

1.2 Neuroanatomy of GWI and Related Neurodegenerative Diseases

1.2.1 The Hippocampus

The human hippocampus (shown in a cutaway drawing in Figure 1) is the subject of many neurological studies of declarative memory and the generation of new memories. Procedural memory, or the acquisition of new motor skills, seems not to be affected by damage to this area. The hippocampus is known to be the central location for spatial memory, navigation, and formation of new memories.

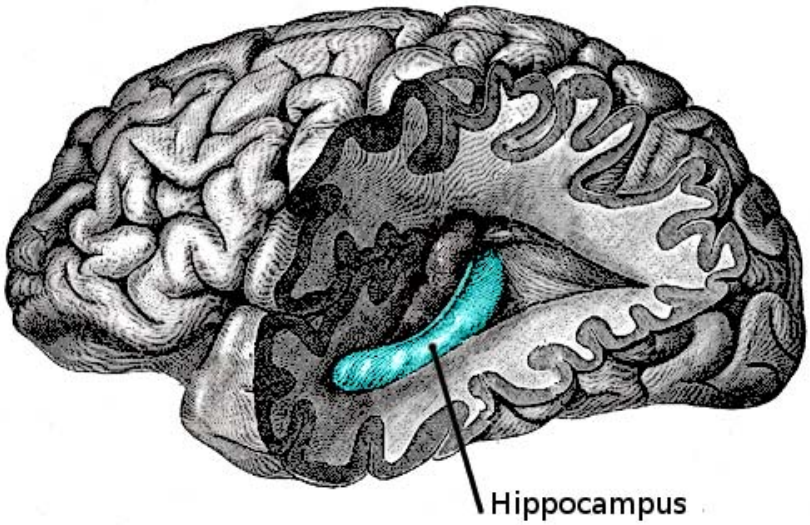

Figure 1. A diagram illustrating the location of the hippocampus, a 3-dimensional, curving structure within the brain. (Gray and Clemente 1985)

In a 2004 proton MRS study of ill Gulf War veterans, Menon et al. postulated that exposure to toxic agents could result in biochemical changes in the hippocampus, due to the high vasculature in that region (Menon, Nasrallah et al. 2004). A trend towards axonal dysfunction, or loss, was found in the GWI group as compared to a control group consisting of non-ill Gulf War veterans. Though the sample size was too small for conclusive findings, the authors conclude that there is evidence of dysfunction related to GWI, and that further investigation in this region of the brain is warranted.

1.2.2 The Pons

The pons is a midbrain structure lying just atop the medulla oblongata adjacent to the spinal cord. A diagram of its location in the brain relative to other structures is shown

in Figure 2. The pons is known to serve as a relay for sensory information and motor control, as well as regulating respiration and other autonomic functions.

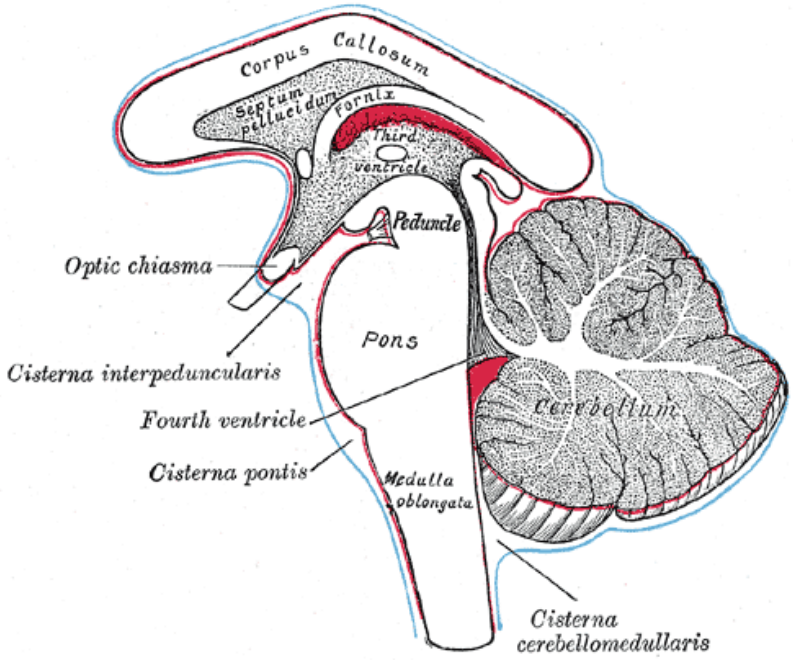

Figure 2: An illustration describing the location of the pons relative to nearby brain structures. (Gray and Clemente 1985)

In the 1998 study of GWI patients, Haley et al. found significant changes in audiovestibular test results as compared to normal controls (Roland, Haley et al. 2000), and followed up with an investigation utilizing proton magnetic resonance spectroscopy in the pons area (Haley, Marshall et al. 2000). In patients with greater vestibular dysfunction – considered most severe in the Syndrome 2 classification of GWI – a greater reduction in neuronal mass was found as compared to less impaired GWI patients and normal controls, as evidenced by a reduction in NAA/Cr_t levels.

1.2.3 The Basal Ganglia

The basal ganglia (grey matter) and the internal capsule (white matter) together comprise the corpus striatum. The amygdale is not always considered a part of the basal ganglia structure, and thalamus is not considered to be part of the basal ganglia structure. A brief cartoon of the shape of the basal ganglia and neighboring thalamus structures is given in Figure 3.

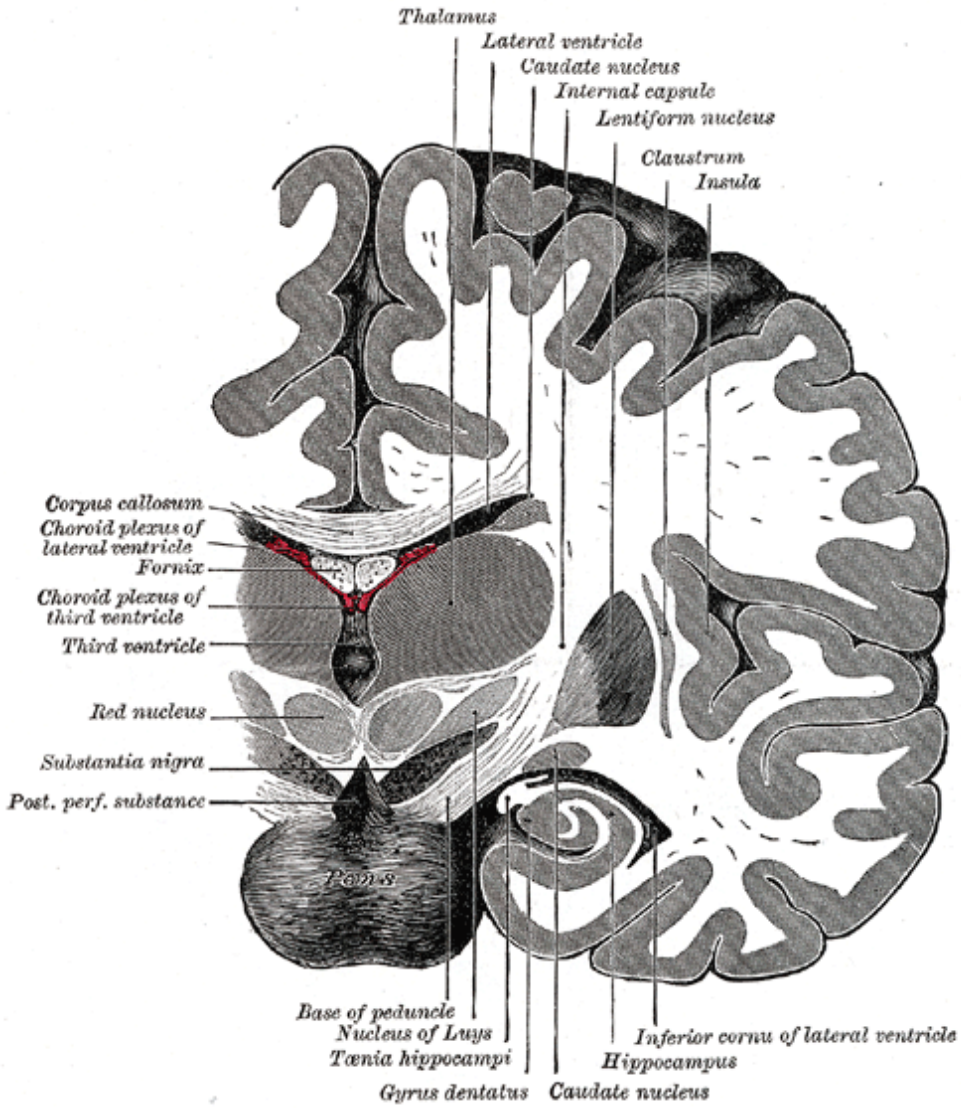

Figure 3: A diagram of the basal ganglia and thalamus in relation to one another and other relevant structures in the brain. (Gray and Clemente 1985)

The human basal ganglia includes several clinically important nuclei – the caudate nucleus, substantia nigra and lenticular nucleus (consisting of the putamen, and globus pallidus) – implicated in a number of neurological disorders (Graybiel 2000; Haley, Fleckenstein et al. 2000; Chaudhuri, Condon et al. 2003; Montgomery 2007; Grahn, Parkinson et al. 2008; Kopell and Greenberg 2008). It is thought to be a filter of cortical inputs, a series of competing pathways designed to either inhibit or excite neuronal activity to control fine motor movement and cognitive tasks. The basal ganglia is widely investigated in studies of major depression, bipolar disorder, and other psychiatric diseases (Kato, Hamakawa et al. 1996; Renshaw, Lafer et al. 1997), however, the majority of basal ganglia research falls in the realm of neurodegenerative diseases. Damages to these pathways have been identified in disorders such as Parkinson's and Huntington's diseases, both marked by symptoms of either excess or paucity of movement. Other disorders that have been found to be related to the basal ganglia include cerebral palsy, foreign accent syndrome, Tourette's disorder, and Wilson's disease. The basal ganglia nuclei are also a focal site for treatment and therapy such as deep-brain stimulation treatment of Parkinson's disease. The loss of tissue volume in this area has also been used as a marker for Alzheimer's disease.

Because of the similarity of symptoms and certain genetic markers described above, several similar neurodegenerative disease models for Gulf War Illness have been suggested, including Parkinson's, Huntington's, Wilson's, and Fahr's. These degenerative diseases are hallmarked by changes in mood, behavior, and cognitive ability

in early onset, before quantitative measurements can identify neurological changes, and later known for neuronal degradation in the basal ganglia region. Specifically, Huntington's disease affects the caudate nucleus, Wilson's begins in the putamen, and Fahr's calcifies the globus pallidus. Unfortunately, while these are all progressive diseases that may eventually be identifiable in MRI images or other imaging modalities, GWI has been postulated to be the result of a specific neurotoxic chemical exposure event, or series of events, which no are no longer contributing to further neurological damage that may be seen by common techniques. This is an added challenge, however, the large foundational research into the diseases previously mentioned greatly helps guide and inform directions for GWI research.

1.3 Spectroscopy in GWI and Related Neurodegenerative Diseases

1.3.1 The Chemical Shift

Proton magnetic resonance spectroscopy (^{1}H MRS) offers valuable information on such diffuse brain pathologies and their mechanisms due to the unique nature of the metabolic information in precise locations within the brain anatomy. A conventional MRI is the result of surveying the density of protons in the abundant chemical species in the body, primarily water and fat.

With a gyromagnetic ratio (γ) of 42.58 MHz/T, protons resonate (flip between two discrete energy states) at 127.8 MHz in a 3 Tesla magnet. This resonance frequency, defined by the Larmor equation,

$$\omega_0 = \gamma_0 \cdot B_0 \qquad \text{(Equation 1-1)}$$

is not exactly the same for all molecular compounds involving protons. The movement of the electrons in the uniform B_0 magnetic field of the magnet creates an additional magnetic field (via Faraday's law) that works to oppose, or shield, the nucleus from the overall B_0 field.

$$B(nucleus) = B_0(1-\sigma) \qquad \text{(Equation 1-2)}$$

The magnetic field at the nucleus is a result of the applied magnetic field (B_0) adjusted by (1-σ), where σ is the chemical shielding term for the nucleus, which depends on the electronic configuration around the nucleus. This slight effect of changing the actual magnetic field experienced by nuclei in different molecular configurations, such as in water (H_20), N-acetyl aspartate (NAA, molecular formula $C_6H_9NO_5$), creatine (Cr, molecular formula $C_4H_9N_3O_2$), and choline (Cho, molecular formula $C_5H_{14}NO^+$), causes the protons in these different chemical moieties to resonate at different frequencies in a fixed and homogeneous magnetic field. It is this fundamental property that allows a standard clinical magnet to be used to detect and quantify these metabolites in the human brain, since the area under the peak is reflective of the number of protons detected in that voxel at that frequency. Fortuitously, the brain is generally free of contaminating signals from lipids, and motion artifact due to the lungs and heart is also minimal in the brain

regions. A standard reference molecule, tetra-methyl silane (TMS) is used to as the zero chemical shift reference from which other resonance frequencies are measured. TMS is an inert, easily removed, and perfectly symmetric molecule that allows for easy, unambiguous frequency locations, given in parts-per-million (ppm). In organic solutions, it is incorporated as an internal reference. In other cases, it is used either as an external reference in a separate tube or capillary, or as an indirect reference, with another peak assigned a chemical shift relative to TMS from prior calibration measurements.

1.3.2 Relevant Metabolites

N-acetylaspartate, located at approximately 2.02 ppm, may include small contributions from N-acetylaspartylglutamate (NAAG). It is considered a marker for neuronal integrity and is reduced in disease processes which result in any number of cognitive impairments. It is the most abundant metabolite visible on a proton spectrum, and is abnormally elevated only in some very few cases, including Canavan's disease (Certaines, Bovée et al. 1992). For all other measured diseases, such as stroke, dementia, and tumors, NAA is markedly decreased. The loss of NAA may be related to loss of neuronal cells, axons, or dendritic structures, as well as a reduction in myelination.

Total creatine, located at approximately 3.0 ppm, is comprised of overlapping signals from phosphocreatine (PCr) and creatine (Cr). In this study, we will designate this total creatine signal by the symbol Cr_t as utilized in other publications (Choi, Coupland et al. 2006). Traditionally, total creatine has been used as a reference for relative quantitation of other metabolites, or used in ratios for normalization, due to the

relative consistency of its concentration across brain areas and physiological conditions, however, recent studies (Ferraz-Filho, Santana-Netto et al. 2009) have shown evidence of changing total creatine levels in malignant tumors and gliomas, which raises the possibility of changing total creatine in other pathologies as, well.

Total choline, located at approximate 3.2 ppm, is considered an indicator of cell membrane viability. The Cho_t signal is comprised of a sum of signals from phosphocholine, free choline, and glycerophosphocholine, by-products of cell membrane breakdown. Cho_t is known to be elevated in dementia, tumors, and multiple sclerosis, as well as in normal aging.

The three metabolites described above are the primary ones under study using current MRS techniques, however, others metabolites present with lower signal strengths, such as lactate, glutamate, and glutamine are increasingly investigated in studies involving other disease models, areas of the body, or magnetic field strengths – as higher-field magnets become more widely available, providing increased sensitivity and spectral dispersion. As many as 25 different metabolites have been studied in the human body (Van Zijl and Barker 1997; Choi, Dimitrov et al. 2009), though NAA, Cr_t, and Cho_t are the most established in the literature, as they represent the highest proton signal in an average brain spectrum after the water resonance.

1.3.3 Spatial Localization of MR Signals in Single Voxel Spectroscopy

A timing diagram for a point resolved spectroscopy (PRESS) sequence, developed by Bottomley, et al. (Bottomley 1987) is shown in Figure 4. A chemical shift selective saturation (CHESS) pulse is first used to suppress water signal. A 90-degree rf pulse excites a slice in the x direction, selected with gradient G_x. A second rf pulse of 180-degrees at time $TE_1/2$, selected by the G_z gradient. This 180˚ pulse rephases the spins that reside in the intersection between the two selected slices and thus creates an echo at time TE_1, however, this echo is not sampled. Finally, a third 180 degree rf pulse and gradient G_y selects a final slice, and only spins in the intersection of all three of these slices (i.e. a single voxel) provide the final echo at time $TE_2/2$ from the third and final 180˚ pulse.

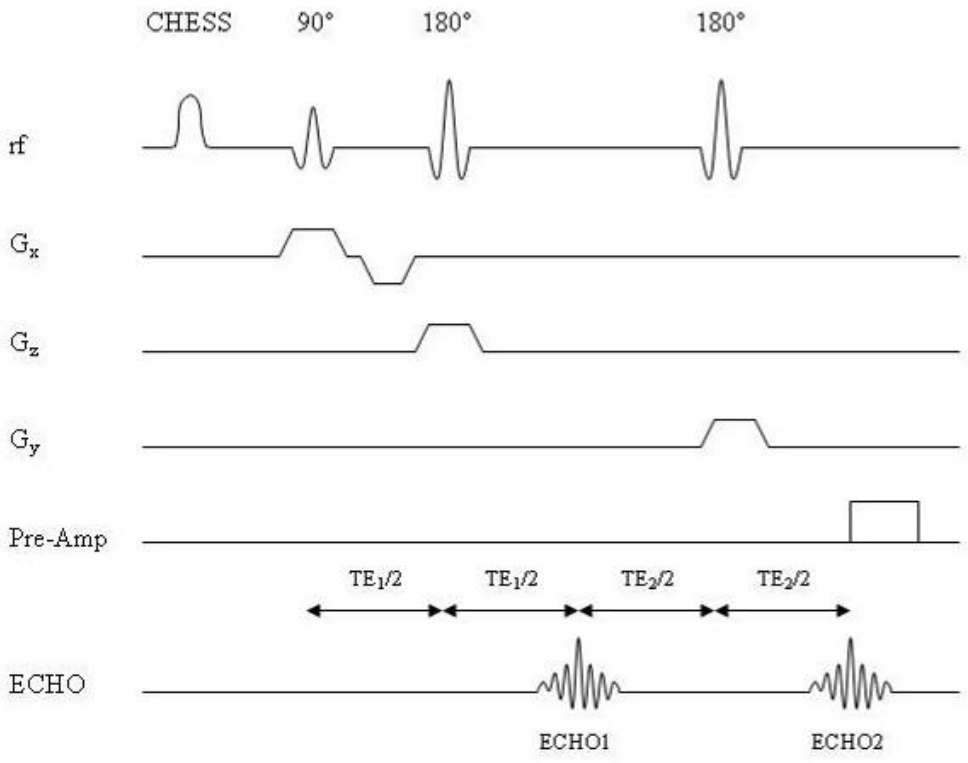

Figure 4: Timing diagram for point resolved spectroscopy sequence (PRESS)

The timing diagram of the stimulated echo acquisition mode (STEAM), developed by Frahm, et al. (Frahm, Bruhn et al. 1989) is similar in nature, however the rf pulses used are three 90-degree pulses, instead of the 90˚-180˚-180˚ sequence.

1.3.4 MRS in Neurological Disorders

The nature of GWI and other neurodegenerative diseases that are not readily apparent on clinically available imaging modalities drives new research into alternative methods for use in detection and diagnosis of these pathologies. In the case of multiple

sclerosis (Richards 1991; Narayana 2005; Zivadinov and Leist 2005), symptomatic lesions that correlate with both prognosis and disability are often invisible on conventional MRI. Conversely, lesions that are visible on MRI correlate only weakly with disability or symptom load. Similarly, Menon et al. found indications of neuronal loss in patients with AIDS via proton spectroscopy in MRI-normal areas (Menon, Baudouin et al. 1990). These are only a few of the examples of using proton magnetic resonance spectroscopy in diseases where obvious abnormalities in MRI do not exist – conventional MRI and other similar imaging techniques, after all, reveal only physical changes to structures inside the brain. Ross et al., in a review of clinical uses of proton MRS, demonstrates the viability of using spectroscopy for diagnosis in brain tumors, strokes, adult and neonatal strokes, intracranial hemorrhage, inborn errors of metabolism, and diabetes mellitus, among other pathologies (Ross, Kreis et al. 1992). More recently, magnetic resonance spectroscopy has been explored for use in the diagnosis and differentiation of high-grade gliomas and other brain cancers (Weiner, Hetherington et al. 1989; Smith, Castillo et al. 2003; Uysal, Erturk et al. 2005; Kwock, Smith et al. 2006; Pfisterer, Hendricks et al. 2007; Ferraz-Filho, Santana-Netto et al. 2009), in the planning of surgical resection and prognosis for recovery (Preul, Caramanos et al. 1998; Kuznetsov, Caramanos et al. 2003), and even perioperative methods (Hall and Truwit 2008). MR spectroscopy has also become a critical tool in the investigation of the more subtle mechanisms underlying neurodegenerative disorders such as Parkinson's disease (Choe, Park et al. 1998; Clarke and Lowry 2000; O'Neill, Schuff et al. 2002), Alzheimer's disease (Chen, Charles et al. 2000; Waldman and Rai 2003; Frederick, Lyoo et al. 2004), amyotrophic lateral sclerosis (Martin 2007), and now Gulf War Illness

(Haley, Fleckenstein et al. 2000; Haley, Marshall et al. 2000; Menon, Nasrallah et al. 2004).

1.3.5 1998 SVS Study on GWI

Haley et al. established a significant difference between six Gulf War veterans afflicted with clinically established baselines of "confusion-ataxia," or "Syndrome 2" (Haley, Kurt et al. 1997) and 18 healthy veterans matched for age, sex, and education using *in vivo* magnetic resonance spectroscopy in both the basal ganglia and pons (Haley, Marshall et al. 2000). The data showed a reduced N-acetyl aspartate (NAA) to creatine (Cr_t) ratio in both the right (18% difference, $P<0.001$) and left (9% difference, $P=0.09$) basal ganglia of affected veterans as compared to the controls, and a 26% reduction in NAA/ Cr_t ratio ($P=0.26$) in the pons region.

The 1998 Haley study used long echo times (TE=272ms). At 1.5T, this is a common technique to minimize baseline contamination from unwanted signals, which would decay at a more rapid rate than the metabolites of interest (NAA, Cr_t, and Cho_t). Using a higher strength magnet, we have been able, in this study, to obtain high resolution, well-resolved spectra at short TE. However, there is still another factor to be considered with varying TE. The relaxation times, assumed to be unchanging in many other studies, have potential to be varying in GWI as well as other neurodegenerative diseases. Relaxation time differences between ill and healthy subjects can affect concentration values – more dramatically at longer TE times, as discussed below. In order to verify the earlier results by Haley et al. it is necessary to confirm the effect of

transverse relaxation times on concentration values. Also, by establishing a protocol to investigate this factor, we may move closer to absolute quantitation of metabolite concentrations.

1.4 Relaxation Measurement

1.4.1 Longitudinal (T_1) Relaxation

Longitudinal relaxation, also referred to as spin-lattice relaxation, or simply abbreviated as T_1 relaxation, occurs after the spins have been perturbed by sufficient resonant rf energy absorption. The magnetization is rotated into a transverse plane by the application of an rf pulse, but then slowly return to their original state by releasing the absorbed energy, following an exponential recovery, described in Equation 1-3 for a 90-degree pulse.

$$M_z = M_0(1 - e^{-t/T1}) \qquad \text{(Equation 1-3)}$$

In the above equation, M_0 is the thermal equilibrium magnetization, M_z is the z component of magnetization at time *t*, and T_1 is the time needed to recover the equilibrium z component of the magnetization vector by $(1\text{-}e^{-1})$, or approximately 63%. After three periods of T_1, the signal has recovered to 95% of its original amplitude; thus, by using a relatively long repetition time (TR), effects of T_1 variations can be largely

disregarded. Even a 20% change in T_1 times will result in less than a 1% change in signal at long TR – usually defined as approximately 3 times the T_1 time.

1.4.2 Transverse (T_2) Relaxation

Transverse relaxation, also referred to as spin-spin relaxation, or simply abbreviated as T_2 relaxation, refers to the loss of coherence of spins initially aligned in the transverse, or xy, plane after a 90-degree pulse. T_2 is specifically known as the time needed to reduce the magnitude of transverse magnetization by a factor of e, as shown in Figure 5.

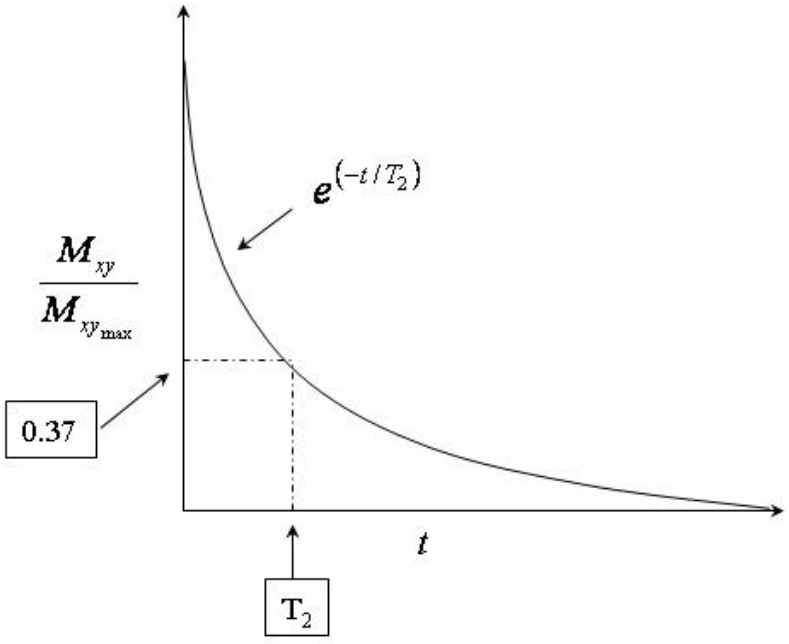

Figure 5. Diagram of spin-spin relaxation and the definition of T_2.

Although initially aligned by a 90 degree pulse, spins begin to magnetically interact with one another, modulated over time by molecular motions, causing each individual spin to precess at a slightly different rate from the others which make up the overall magnetization vector. This causes the transverse magnetization to decay. At time *t* approaching infinity, the spins have completely returned to a completely random state, thus the overall magnitude of the xy magnetization vector M_{xy} approaches zero. The exponential reduction of the magnitude of M_{xy} is given in Equation 1-4.

$$M_{XY} = M_{XY0}(e^{-t/T_2}) \qquad \text{(Equation 1-4)}$$

In conventional MRI investigations, the echo time TE and the recovery time TR are set to create signal contrast among different tissue types with different T_2 and T_1 relaxation times.

For MR data collected under partially relaxed conditions (TR < 3-5 T1, TE > 0.2 T_2), estimation of metabolite concentrations (either absolute concentrations or ratios) can be confounded by differences in or changes over time in relaxation times. The individual metabolite relaxation time measurements affect the ability to detect significant changes in cerebral metabolite concentrations over time. In addition to metabolite concentration corrections, information about variation in metabolite relaxation times might provide insight into molecular mechanisms of disease progression. A shorter measured T_2 in tissue may indicate increased restriction of molecular movement, or increased amounts of paramagnetic species such as iron or manganese ions. Several studies have reported decreased T_2 times in such disease states as Parkinson's and Huntington's, speculated to be a result of increased iron and ferritin deposits in the putamen and substantia nigra

regions (Antonini, Leenders et al. 1993; Chen, Hardy et al. 1993). Finally, when comparing groups of subjects, such as veterans ill with Gulf War Syndrome and normal controls, relaxation times can serve as diagnostic markers to differentiate groups and monitor disease progression or regression.

A hypothetical 20% reduction in metabolite T_2 times – from 221ms to 177ms, the T_2 value established in an NAA grey matter voxel by Traber et al. at 3T (Traber, Block et al. 2004) – results in approximately a 2% change in resulting signal at TE of 30ms, but at a TE of 270ms (or 272ms, as in the case of the 1998 Haley study), the change in metabolite concentration can be affected by up to 8%.

1.4.3 Measuring Transverse Relaxation in the Brain

The Mlynarik et al. paper was one of the first studies of T_2 relaxation values at 3T in different brain regions in normal control subjects. Mlynarik et al. (Mlynarik, Gruber et al. 2001) also investigated T_2 relaxation times between 1.5T and 3T in brain regions, however, only investigated occipital white and occipital grey matter voxels. Using a STEAM protocol in a 2x2x2 cm^3 occipital grey matter voxel with TE = 50/100/150/200/250 ms, they found T_2 values (± SE) of 295±29 ms for NAA, 156±20 ms for Cr_t, and 187±20 ms for Cho_t (group average, N=5).

Barker et al. (Barker, Hearshen et al. 2001) also compared 1.5T and 3T T_2 time differences, using a STEAM sequence in a 2x2x2 cm^3 voxel located at random in the right or left centrum semi-ovale. Using TE = 20/67/136/272 ms on the same 5 normal

control volunteers on two different scanners (a 1.5T General Electric Signa Horizon Echospeed and a 3T Surrey Medical Imaging System), Barker et al. confirmed previous literature findings of decreased T_2 times from 1.5T to 3T, and a 20% increase in sensitivity at 3T at short echo times (TE=20ms). T_2 values (± SD) were given as 0.21±0.02 seconds for NAA, 0.15±0.04 seconds for Cr_t, and 0.18±0.04 seconds for Cho_t (group average, N=5).

These studies are mainly useful for establishing the different T_2 relaxation times from 1.5T to 3T systems. There is no standard for measurement in acquisition or post-processing of T_2 data, and there is still some dispute on acceptable techniques for accurate measurements. Some recent studies have begun using a two-point optimized method proposed by Fleysher et al. to determine T_2 (Fleysher, Fleysher et al. 2007), however, by fitting a line to two points, the quality of line fit cannot be determined. Other recent studies (Tsai, Posse et al. 2007; Zaaraoui, Fleysher et al. 2007) have used chemical-shift imaging (CSI) to increase spatial coverage and maximize resolution, but in this case, shimming and homogeneity is lost along with SNR.

As discussed in a note from Whittall, MacKay and Li, in the majority of T_2 relaxation studies, an insufficient number of echoes are used to determine T_2 times accurately (Whittall, MacKay et al. 1999). Also, the authors attempt to show, through simulated studies, that fitting data to mono-exponential curves is responsible for errors in previous claims that T_2 relaxation times of water in white matter is less than that of grey matter – the mono-exponential fit underestimates true T_2 times by not taking into account T_2 contributions from other components or partial volumes. In another simulation, a

controlled amount of CSF contamination was introduced into a gray matter calculation of T_2 times. The 4-echo mono-exponential fit now overestimated T_2 due to the long T_2 time contribution of the CSF water. In the *in vivo* data collected by Whittall et al., they estimate CSF contamination of grey matter voxels to be anywhere from 1 to 15 percent, which, according to their simulated data, could result in overestimation errors in grey matter of 1% (for CSF contamination of 1%, 4 echoes, and mono-exponential fits) to up to 38% (for CSF contamination of 15%, 4 echoes, and mono-exponential fits). Finally the authors investigate the various TEs used in the acquisition and conclude emphatically that the oft-used 2 echoes for T_2 fits generate misleading results. According to the simulated studies of several typical TE choices from current literature, there was up to a 15% error in resultant T_2 times.

Although these observations were made from simulated studies, and modeled after water, not metabolite T_2 times, there are important errors to be considered in T_2 relaxation time measurements emphasized in this note. The three key areas for error as defined by Whittall et al. are: 1) inherent multi-exponential relaxation time components, 2) external relaxation time component contributions from partial volumes, and 3) insufficient time points for decay curve calculations. The methods to minimize these errors, as recommended by Whittall et al. are to perform spectroscopy studies in 1) grey matter areas known to not have multiple relaxation time components, 2) are highly homogeneous, and 3) obtain regression fits with greater than 4 TE samples.

As for metabolite T_2 relaxation times measured *in vivo* in the brain, Traber et al. found no evidence of multi-exponential behavior, despite explicitly implementing an

extended PRESS protocol with >7 TE values, ranging from TE=30 to 400ms, in all investigated brain regions (Traber, Block et al. 2004). The data was fit well (7% fitting accuracy for Cr_t group data, and 2-3% for the other investigated metabolites) using mono-exponential decay curves and 4 TE values of 280 ms or less. Comparing their results with and without inclusion of the longer TE values (TE>280ms) did not significantly change the resultant T_2 times (<1% difference for means of NAA and Cho_t, 2.2% decrease for Cr_t). With the 30ms TE value, however, the regression line in the semi-logarithmic plot was distorted, and thus the TE=30 ms point was disregarded in regression calculations. This deviation from the mono-exponential decay is explained by Traber as contribution from the Glx (glutamate and glutamine) complex signal artificially elevating the NAA signal.

In the basal ganglia voxel used by Traber et al. (3x2.5x2 cm^3), at TE = 50/120/200/280/400 ms, they found T_2 values (± fit errors) of 221±18 ms for NAA, 143±13 ms for Cr_t, and 201±16 ms for Cho_t (group average, N=8). These T_2 values are significantly lower than the values in the same study for other brain regions for all three metabolites, including occipital white matter, cerebellum, and fronto-lateral white/grey matter.

2 PURPOSE

While one of the main goals of the Gulf War study conducted at UT Southwestern was to replicate previous findings by Haley et al. (Haley, Marshall et al. 2000), the large patient population under study presents a rare opportunity to establish new protocols for investigating subtle physiological changes in neurodegenerative diseases as a whole. Our aim in this large research collaboration is to discover new insights into the mechanisms underlying Gulf War Illness, and to guide and inform future diagnosis, therapy, and management.

The purpose of this study, within the larger confines of the more general Gulf War Illness study, is to measure the transverse (T_2) relaxation times of the major brain metabolites (NAA, Cr_t, and Cho_t) to determine if the T_2 values differ between veterans with Gulf War Illness (GWI) and age-matched normal controls. Furthermore, it is necessary to investigate if T_2 relaxation values differ amongst the Haley-defined syndrome classifications. This knowledge can clarify whether the reported significant changes in metabolite concentrations are due to true changes in concentration, or changes in signal intensity caused by significantly changed transverse relaxation times in illness.

To achieve this aim, it will also be necessary to establish a technique that is both reproducible and sensitive to potential metabolite T_2 relaxation time changes in neurodegenerative diseases *in vivo*.

2.1 Specific Aims and Hypothesis

Transverse relaxation time changes in neurodegenerative diseases such as Parkinson's and Huntington's have been observed in several studies (Antonini, Leenders et al. 1993; Chen, Hardy et al. 1993). These changes have been speculated to be a result of increased iron and ferritin deposits in the putamen and substantia nigra regions (Gelman, Gorell et al. 1999; Brass, Chen et al. 2006; Mitsumori, Watanabe et al. 2007; Mitsumori, Watanabe et al. 2009). Because of similarities in symptoms of Gulf War Illness and these diseases, it is expected that similar changes in T_2 may occur for GWI.

Additionally, the previous spectroscopy studies done in GWI (and many other similar disease models) to quantify metabolites have not accounted for possible variations in T_2 or T_1 relaxation times. Significant differences in metabolite ratios seen in previous studies may be attributable, in part, to altered T_2 values, instead of differing concentrations of NAA or other metabolites. Measurements of T_2 values must be made to move towards absolute quantification of metabolite concentrations in tissue and to thoroughly evaluate this possibility.

2.1.1 Procedural Hypothesis

Hypothesis 1) Transverse (T_2) relaxation time can be accurately and reproducibly measured with widely available single voxel spectroscopy techniques on a 3-Tesla magnetic resonance imaging system, with sufficient signal to noise ratios and sensitivity

for differentiation between expected ranges of values for differences in major brain metabolites (NAA, Cr_t, and Cho_t) *in vivo* within individuals or groups.

Specific Aim 1) Procedures (including voxel placement and shimming) will be developed and tested with the goal of accurately and reproducibly measuring human basal ganglia ^1H T_2 values of the methyl group singlets of the major metabolites NAA, Cr_t, and Cho_t.

2.1.2 Metabolite Transverse Relaxation Variation Hypothesis

Hypothesis 2) Veterans suffering from Gulf War Illness will exhibit different basal ganglia NAA, Cr_t, and Cho_t T_2 values than veteran control subjects. Furthermore, Syndrome 2 is expected to show the largest relaxation time change of the three major Gulf War syndromes.

Specific Aim 2) The NAA, Cr_t, and Cho_t T_2 relaxation times of veterans ill with Haley Syndromes 1-3 will be measured in the basal ganglia and values for Syndromes 1-3 and controls compared.

2.1.3 Concentration Effect Hypothesis

The effects of repeated, low-level organophosphate exposure have been shown in other studies to result in a significant change in the chemical and metabolite composition of the basal ganglia region (Freed, Haque et al. 1976; Freed, Matin et al. 1976; Fernando,

Hoskins et al. 1984; McDonald, Costa et al. 1988). Thus, it is expected that the early degeneration of the basal ganglia tissue in the affected veterans will result in significant biochemical changes in this deep brain structure. Secondarily, it is expected that, due to severity and type of symptoms demonstrated by the different syndromes, that Syndrome 2 ("confusion-ataxia") subjects will demonstrate the most significant biochemical changes as compared to other syndromes and normal controls.

Hypothesis 3) The group differences in NAA, Cr_t, and Cho_t signal intensities attributable to differences in metabolite T_2 relaxation times are not major contributors to the observed differences of metabolite signal intensities between groups.

Specific Aim 3) The metabolite concentrations and ratios estimated from signal intensities will be corrected with the measured T_2 relaxation times to assess the degree to which differences in T_2 contribute to signal intensity differences, and to compare relaxation-corrected values.

3 METHODS

3.1 GWI Research Basis

This study contributes important data to help analyze and interpret MRS data from ill Gulf War veterans compared to controls, and is a part of the MRS Sub-Core for the Gulf War Illness project at UT Southwestern. The goals of the MRS Sub-Core are three-fold: 1) to reproduce significant findings from the 1998 Haley study (Haley, Marshall et al. 2000), 2) to expand and improve upon these established techniques to move toward an absolute method of quantitation of cerebral metabolites *in vivo* by first creating a reliable protocol for detection of T_2 relaxation times, and 3) to specifically quantify the extent to which T_2 relaxation differences between ill Gulf War veterans and normal controls are affecting concentration calculations in brain metabolites.

3.1.1 Reproduction and Expansion of the 1998 GWI Study

The first goal of the overall GWI research study was to re-establish findings from the original Haley study (Haley, Marshall et al. 2000) performed in 1998 on veterans returned from the first Gulf War.

This study was meant to be exploratory in nature – as mentioned in the discussion, robust statistics await confirmation from a larger subject pool before these results are applicable to diagnosis in future patients. Establishing differences not only between ill and non-afflicted veterans laid important groundwork for future studies, the

added significance between the syndrome classifications further supported the hypothesis of differing chemical exposure profiles for each symptom classification.

However, a true longitudinal study was technically impossible, as the hardware in the intervening ten years had advanced considerably, and the original 1.5 Tesla Philips Gyroscan NT MR imager was no longer available for use. The magnet used in this study is a 3T Siemens Tim Trio magnet system. Although the patient population itself is unchanged, the subjects have aged ten years, potentially confounding the original neurological symptoms with age-dependent effects.

Taking all these changes into account, an amended protocol was favored to optimize parameters, since a strictly longitudinal study on the original population was not possible. A repeat of the single voxel measurement instead of a spectroscopic imaging study was selected because of the increased field homogeneity and precision of voxel placement over the studied areas. The voxel size in the basal ganglia was decreased slightly, from 40x20x20 mm^3 to 30x20x20 mm^3, and was placed obliquely with respect to the localizers, to further minimize effects of partial voluming – structures outside the basal ganglia falling inside the voxel. To aid in the consistent placement of the voxel, high-resolution localizers were acquired, employing the system's AutoAlign feature, for increased reproducibility. The AutoAlign feature included in the Siemens system assists with placement of slices and voxels, by automatically adjusting high resolution localizer display to an averaged template atlas, to which individual subject brain anatomy can be aligned, thus allowing for more accurate and reproducible slice prescription between sessions and across subjects.

The TE times chosen for this study, after optimizing through pilot studies in normal control subjects, were 60, 90, 135, 195, and 270 ms, to minimize errors as discussed in various simulated studies by Brief et al. (Brief, Whittall et al. 2005) while still making efficient use of time allocated to this study within the larger GWI research program from each patient. By using a homogeneous voxel located in the grey matter area of the basal ganglia, confirmed by high resolution localizers, CSF contamination was minimized.

3.2 Subject Participation

A normal control study was performed prior to beginning study on the population of afflicted Gulf War veterans to establish reliability and reproducibility of the measurements, as well as sensitivity and accuracy of techniques. Gulf War veteran data was acquired over a period of a year and one month (June 2008 – July 2009), and syndrome classification/normal control status was not disclosed until after the study was completed.

3.2.1 Normal Control Subjects

Normal control subjects consisted of 8 volunteer participants (25-56 years old, mean age 37.5±10.9 years, 6 male, 2 female, all right-handed). Included control subjects did not report any neurological conditions and MRI data was judged to be normal. Four separate 1.5-hr sessions were performed on each subject to robustly determine both intra-

and inter-subject variability within a time frame of 4 months. Minimum interval between successive sessions was 1 day, and maximum interval was 4 weeks. Both right and left basal ganglia voxel T_2 and metabolite concentration data were measured in each session for each subject, along with pons concentration acquisition, for a separate study not discussed here. In total, each basal ganglia T_2 measurement involved approximately 25 minutes of acquisition time, localizers not included. Each subject was briefed on the procedure and gave written consent prior to examination. The consent form was approved prior to the study by the Institutional Review Board of the University of Texas Southwestern Medical Center at Dallas.

3.2.2 Gulf War Veteran Subjects

Gulf War Veteran subjects consisted of 56 male participants (44-76 years old, mean age 59±7.2 years), from Twenty-fourth Reserve Naval Mobile Construction Battalion (Seabees), the same group from earlier Haley studies described above (Haley, Kurt et al. 1997; Hom, Haley et al. 1997; Haley, Marshall et al. 2000). The groups consisted of: 16 normal veterans from the same deployed construction battalion, matched for age and education, 17 subjects diagnosed with Haley syndrome classification 2 ("confusion-ataxia"), 12 subjects diagnosed with Haley syndrome classification 3 ("arthro-myo-neuropathy"), and 11 subjects diagnosed with Haley syndrome classification 1 ("impaired cognition"). Subjects had two session of approximately 1 hour and fifteen minutes each, in which both left and right basal ganglia T_2 data were acquired, along with pons, hippocampus, and CSI data, for separate analysis not

discussed here. In total, each basal ganglia T_2 measurement was approximately 25 minutes of scan time, not including localizers, and not necessarily occurring during the same session with the subject. After reviewing several normal control pilot studies, it was determined that there was no significant variation in subject data attributable to time of scan or time between scans. Each subject was briefed on the procedure and gave written consent prior to examination. The consent form was approved prior to the study by the Institutional Review Board of the University of Texas Southwestern Medical Center at Dallas.

3.3 MRS Data Acquisition

T_2 relaxation times of N-acetylaspartate (NAA), creatine (Cr_t), and choline (Cho_t) were measured with a 3T Trio TIM system (Siemens AG, Erlangen, Germany), with a center frequency of 123.244 MHz, using a standard issue 12-channel head coil, by a series of standard single-voxel sequences (SVS PRESS: see Appendix for full details) at a TR of 2500 ms and varying echo delay times (TE): 60/90/135/195/270 ms (32 averages (NS) at TE 135 and below, 64 averages at TE 195 and above, to compensate for decreasing SNR at higher TE values). The voxel (20mm x 30mm x 20mm, 12.0 mL) was placed reproducibly in the basal ganglia for each measurement (as shown in Figure 6, Figure 7 and Figure 8) by using the Siemens AutoAlign feature with high-resolution localizers. A voxel of this size, placed as medial and as superior as allowed by the limitation of the ventricles, will consist in the most part (as discussed above and shown in

Figure 9 and Figure 10) of putamen and caudate nucleus (50-70%, depending on individual anatomy), with some (at most 30%) contamination from the thalamus.

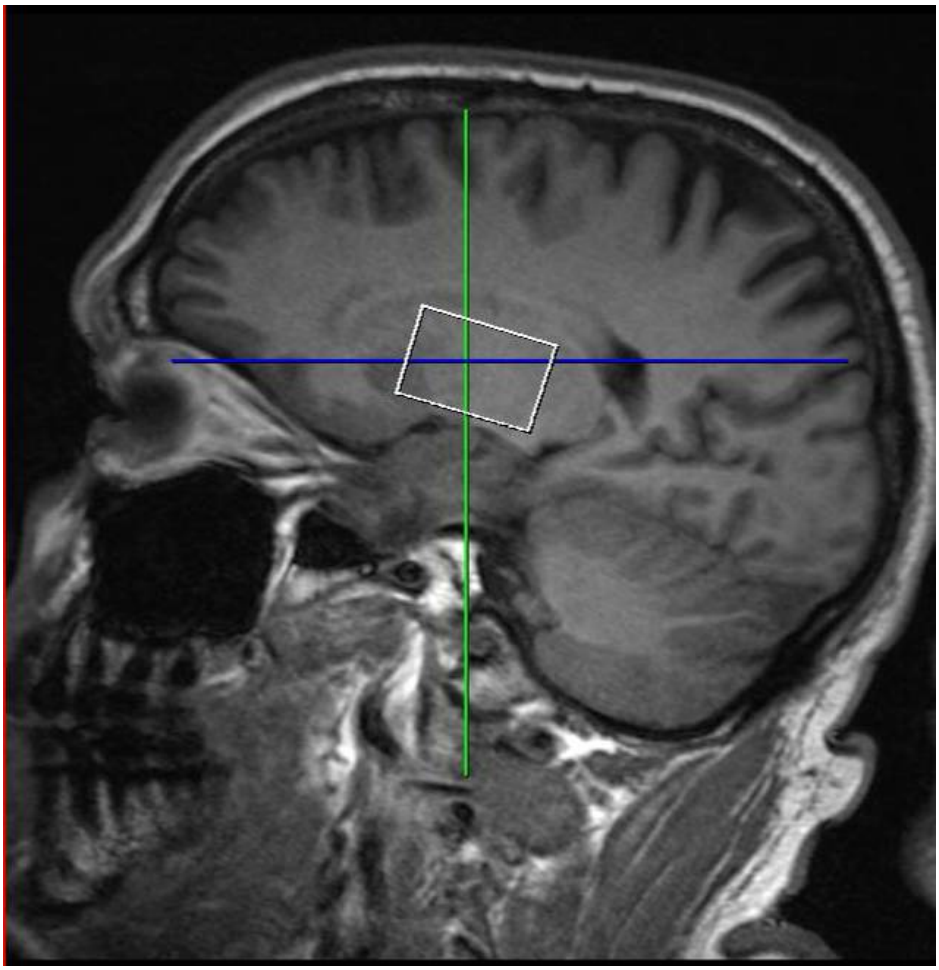

Figure 6: Example placement of left basal ganglia voxel (20x30x20 mm^3) in sagittal T_1-weighted plane.

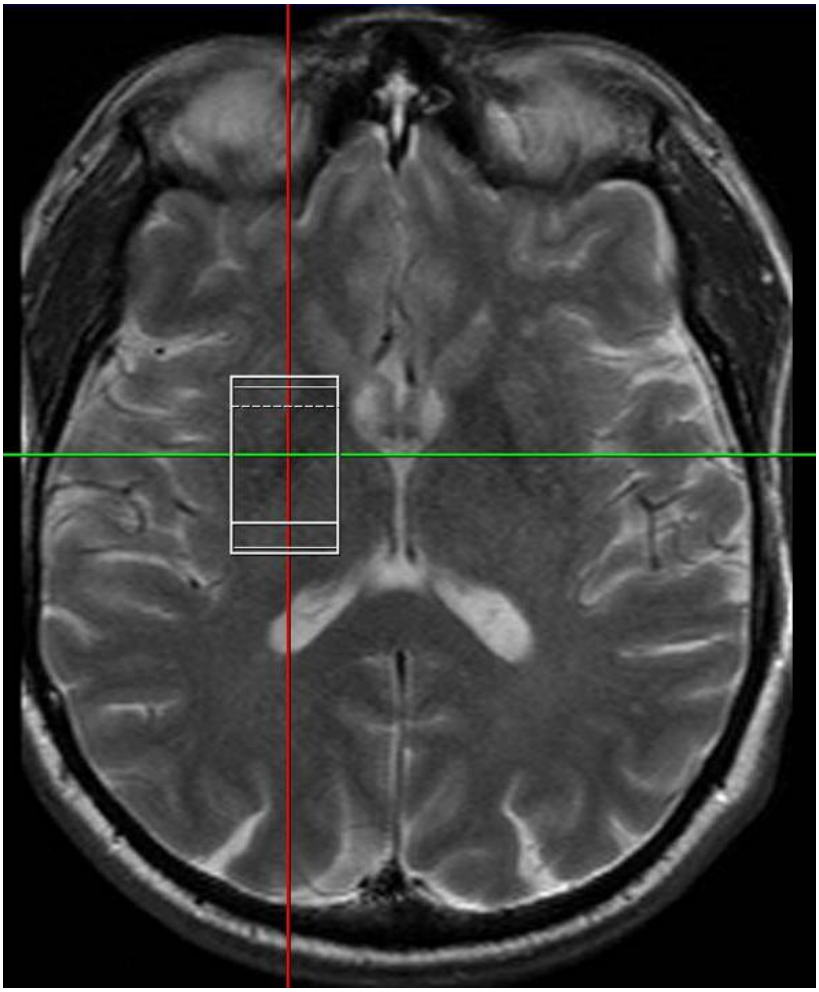

Figure 7: Example placement of left basal ganglia voxel (20x30x20 mm^3) in T_2-weighted image of the axial plane.

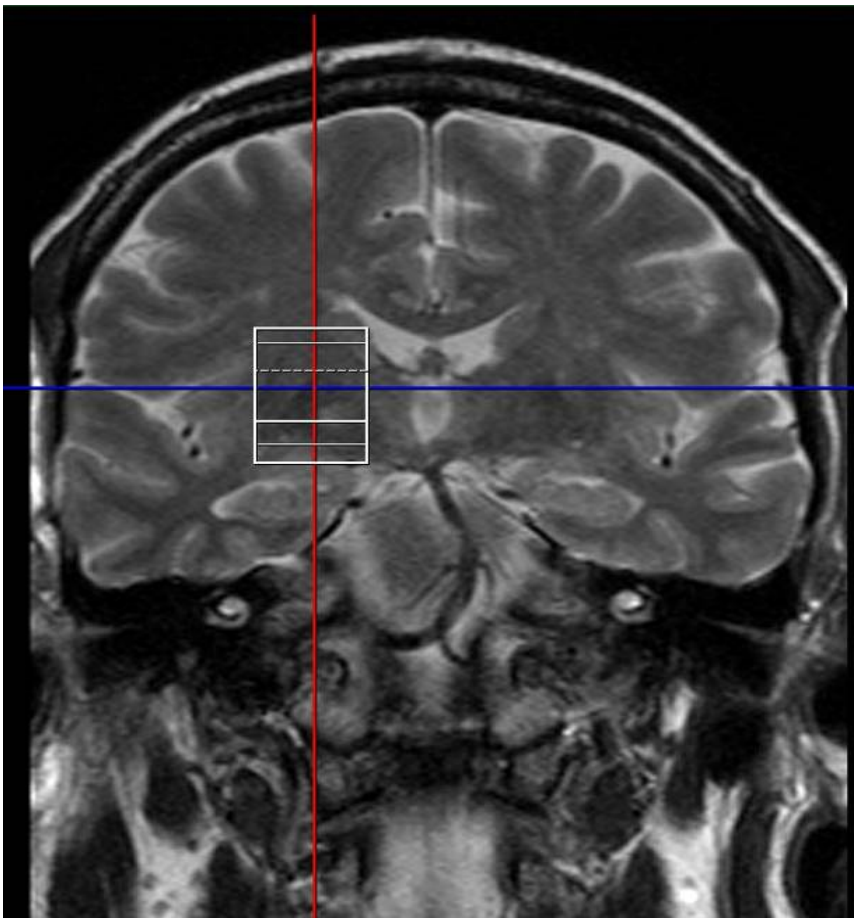

Figure 8: Example placement of left basal ganglia voxel (20x30x20 mm^3) in T_2-weighted image of the coronal plane.

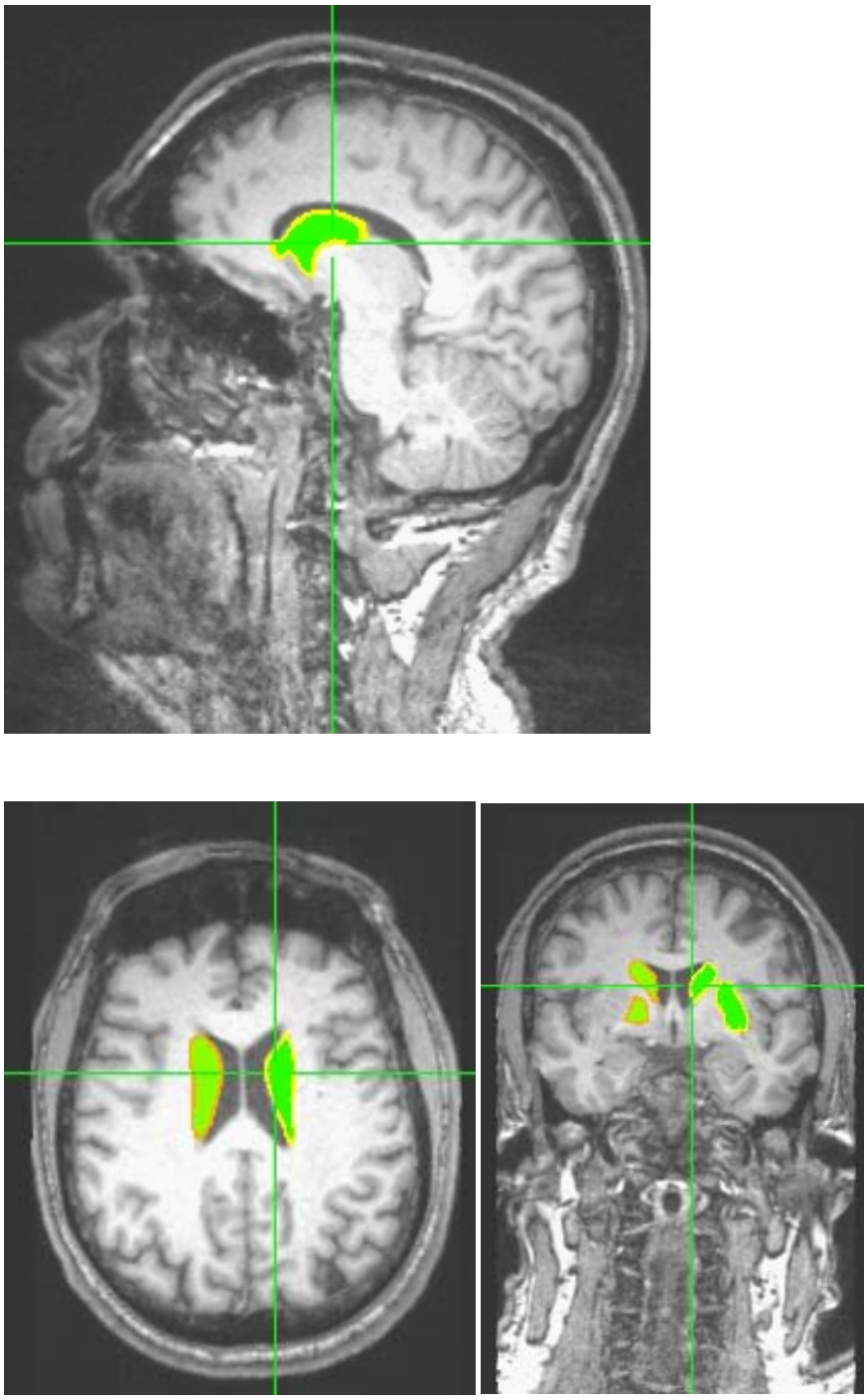

Figure 9. Sagittal, coronal, and axial sections showing caudate head and putamen brain regions highlighted in a typical Gulf War veteran subject.

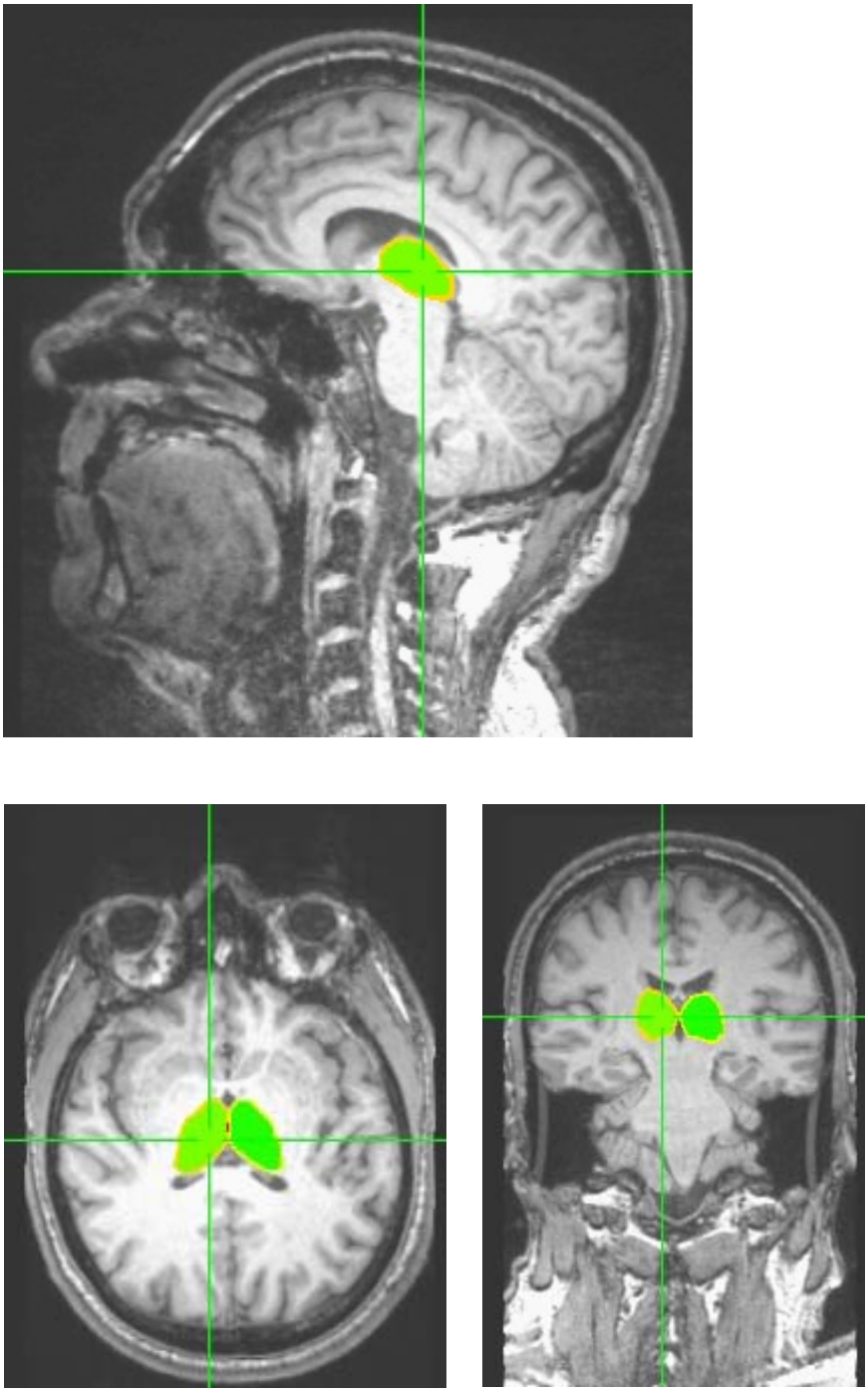

Figure 10. Sagittal, coronal, and axial sections showing thalamus as the highlighted region in an example Gulf War veteran subject.

Thirty-two 4-mm thick T_1-weighted MPRAGE sagittal-plane slices (TE/TR = 2.75/1100) with a 210x210 field of view (FOV) were coupled with 4-mm slice thickness axial and coronal images acquired with T_2-weighted turbo spin-echo sequences (TE/TR = 76/2800, FOV = 200x200). For each subject, the Siemens AutoAlign sequence was used to reproducibly place localizers for each session, and the placement of VOIs were adjusted as needed to achieve minimal partial voluming effects (i.e. voxels placed entirely within basal ganglia structures). First-order shims were manually optimized using the Siemens advanced user adjustments to minimize inhomogeneity in the magnetic field. For each measurement on individual subjects, the raw water half-height line width without any additional line broadening, as reported by the Siemens hardware was approximately 18 Hz at TE=30ms. An example raw spectrum from the Siemens hardware is shown in Figure 11.

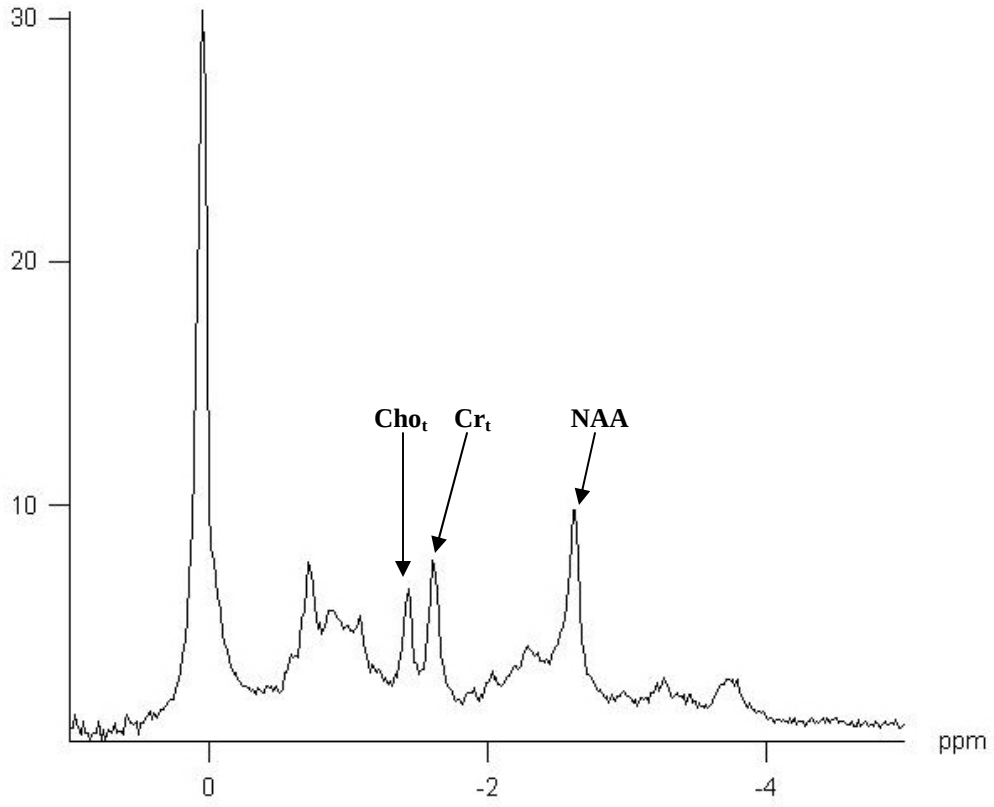

Figure 11. Example magnitude spectrum from the Siemens 3T Tim Trio system interface, shown without post-processing of baseline, apodization, zero-filling, or phase adjustments at TE/TR/NS=30ms/2500ms/96.

Single voxel metabolite concentration determination was made from the same voxel location and same parameters as above, except TE/TR/NS = 30ms/2500ms/96, with an extra unsuppressed acquisition with NS=8 and identical gradient scheme, for eddy current compensation done within the LCModel software via point by point phase correction (Klose 1990; Drost, Riddle et al. 2002) in later processing.

3.4 Spectroscopy Data Analysis

3.4.1 Metabolite Concentration Determination

Post-processing of single voxel metabolite concentration data was performed by Dr. Hyeonman Baek of the MRS sub-core using the QUEST modeling algorithm of the jMRUI (Naressi, Couturier et al. 2001) software package with prior spectral knowledge simulated in NMR-SCOPE using 12 modeled peaks, and by Dr. Sergey Cheshkov of the MRS Sub-Core, using LCModel (Provencher 1993) software, which utilizes prior spectral knowledge of 26 modeled metabolite (including macromolecular species) peaks in basis spectra acquired from in vitro models at the same TE, provided by the vendor. As can be seen in an example spectrum processed with LCModel in Figure 12, several metabolites can be detected with reasonable confidence (as determined by Cramer-Rao bounds) at TE/TR/NS = 2500ms/30ms/96. NAA, Cr_t, and Cho_t metabolite concentrations were established with an average standard deviation of 4% per measurement.

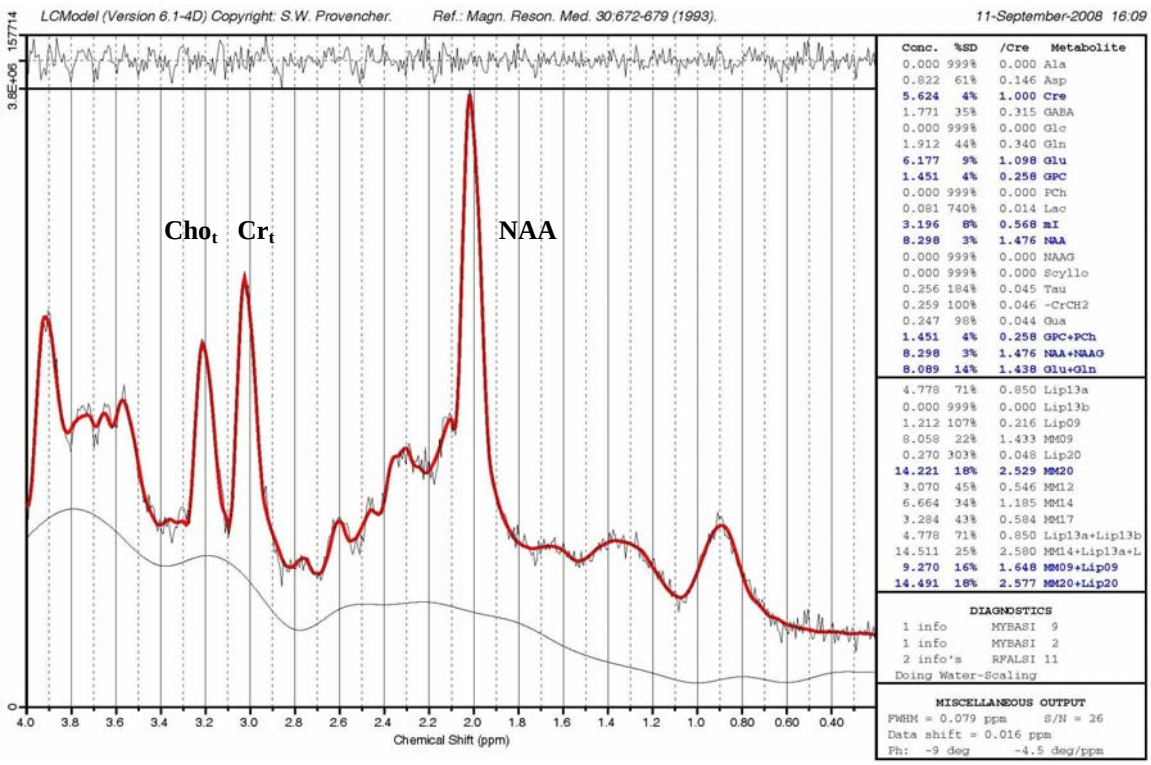

Figure 12. Example of left basal ganglia metabolite concentration data acquired at TE/TR/NS=30ms/2500ms/96 processed in LCModel. Metabolites detected with reasonable confidence (as determined by Cramer-Rao lower bounds) listed in bold font. Courtesy of Dr. Sergey Cheshkov.

3.4.2 Metabolite T_2 Determination

Transverse relaxation analysis consisted of Hankel Lanczos squares singular values decomposition (HLSVD) filtering of the remaining water signal, apodization of 5 Hz, quantification of the three major metabolite signals by the non-linear AMARES algorithm of the jMRUI software package (Naressi, Couturier et al. 2001), and a least-squares fit (not weighted by SNR) to the logarithm of the peak areas vs. echo time. The TE=30ms data point was determined to have excessive baseline contamination, and therefore was not included in the regression calculation. The metabolite signals for NAA, Cr_t, and Cho_t were optimal for investigation due to good quality signal to noise

ratio at all measured TEs. At higher TE values, partial T_1 saturation leads to decreased signal intensity for constant TR paradigms such as was used to collect this data, which if not accounted for leads to systematic underestimation of T_2 values (Lin 1984). The longitudinal relaxation correction factor by which the measured intensity at each TE should be divided is:

$$f(T1,TR,TE) = 1 - 2\exp[-(TR-3TE/2)/T_1] + 2\exp[-(TR-TE/2)/T_1] - \exp[-TR/T_1]$$

(Equation 1-5)

Between TE=30 ms and TE=270 ms, the shortest and longest TE values used in this study, at TR=2500 ms, and utilizing the value of 1.56 seconds as the longest estimated T_1 relaxation value from literature, the correction factor described in Equation 1-5 differs by 3%, and was applied to the calculated T_2 values.

An example spectral fit in jMRUI, using the AMARES algorithm and appropriate prior knowledge (as determined by pilot studies) is shown in Figure 13. Example spectra at TE=60/90/135/195/270 ms are shown in Figure 14, and the accompanying linear regression plot is shown in Figure 15.

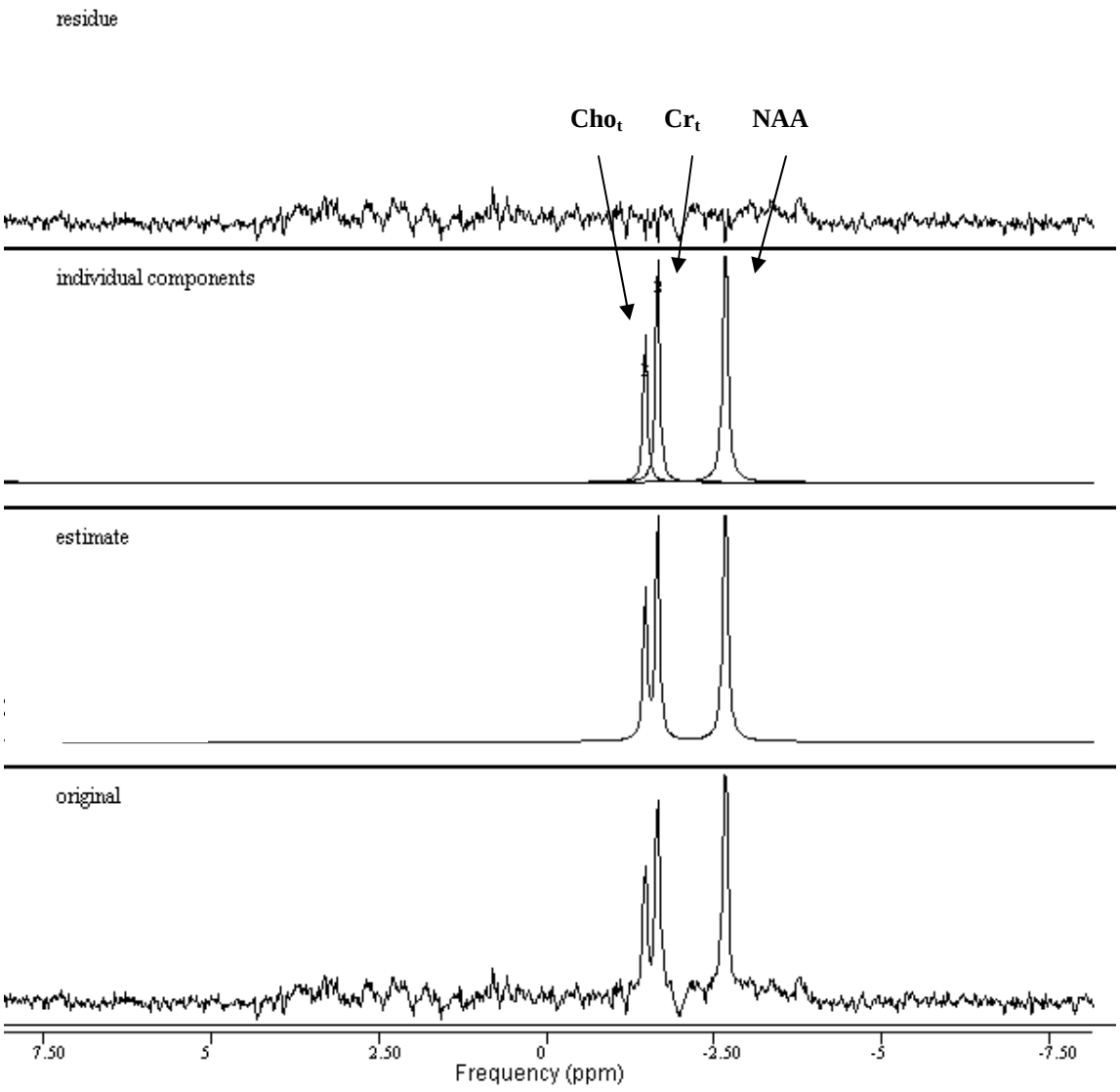

Figure 13. An example of spectral fit of a veteran left basal ganglia acquired at TE=60 ms in jMRUI, using the AMARES quantitation algorithm, showing the original signal, after 5-Hz apodization and HLSVD removal of water signal, estimate of the 3 modeled metabolite peaks, and residual signal after individual components are removed.

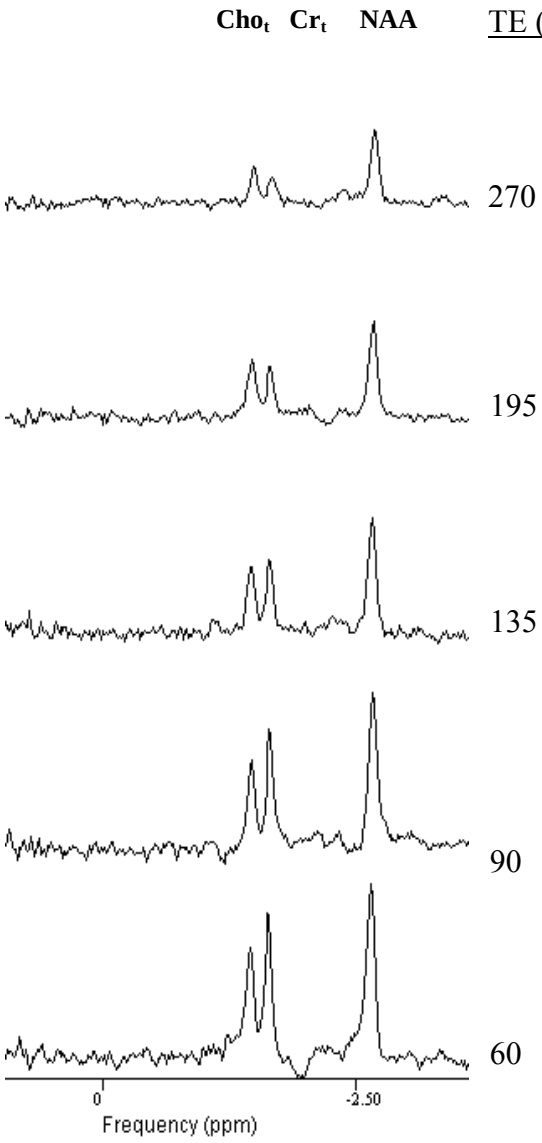

Figure 14: A series of example spectra after 5-Hz apodization from the right basal ganglia of a typical subject with varying echo times.

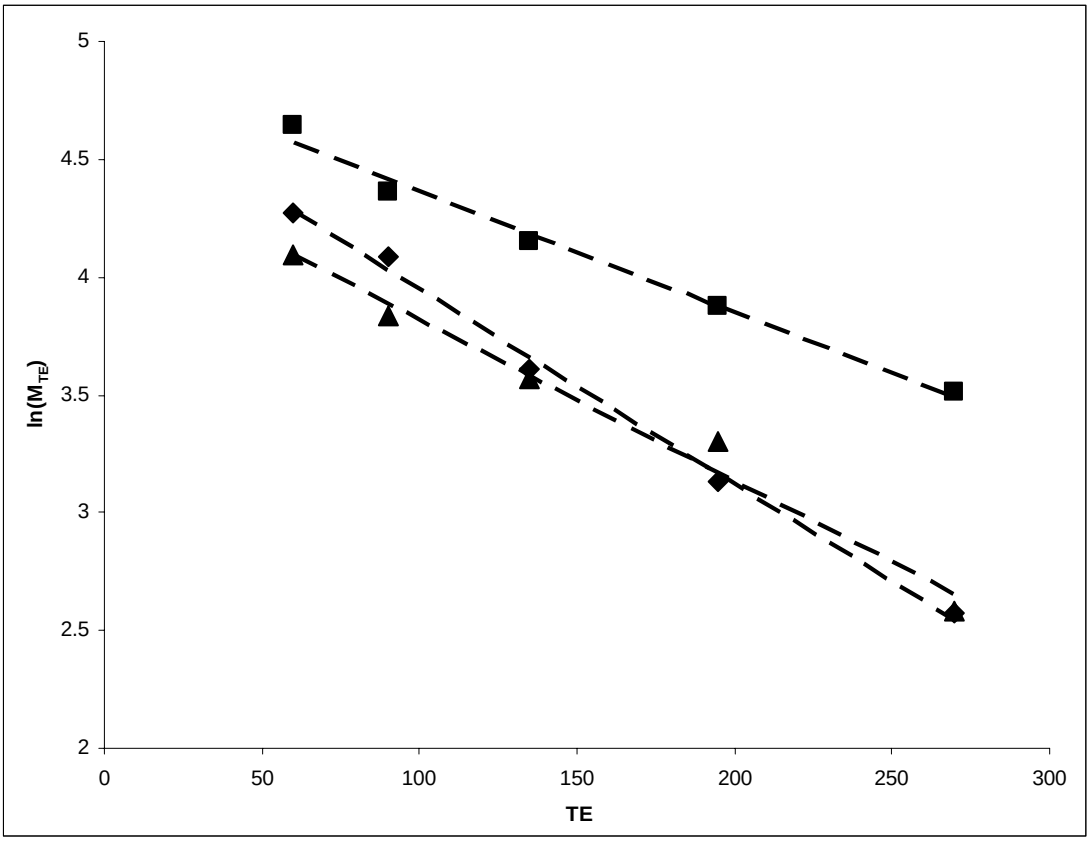

Figure 15: The accompanying signal decay plot to the right basal ganglia spectra in Figure 14. The dotted lines represent estimated least-squares line fit to the line area data.

4 RESULTS

4.1 T_2 Measurement Reproducibility of Normal Controls

The first goal of this study was to develop procedures to accurately and reproducibly measure human basal ganglia ^1H T_2 values of the major brain metabolites (NAA, Cr_t, and Cho_t) using the pre-existing hardware and scan time limitations.

All 64 (8 basal ganglia measurements, 4 time points each for left and right basal ganglia, for each of the 8 normal control subjects) T_2 measurements obtained in this study on normal controls showed good resolution of the three major metabolite peaks and therefore were deemed of sufficient quality for use in analysis. Because one of the overall objectives of the normal control reproducibility study was to develop specific methods on the current hardware to obtain reliable results, no spectra were to be excluded unless the peaks could not be resolved by the AMARES quantitation methods. Extensive piloting of the methods proved that the spectra could be obtained in such a way that no acquisitions would be lost due to poor resolution of peaks.

No significant difference was found in comparing left to right basal ganglia T_2 values (displayed in Figure 16) using two-tailed paired statistical testing. Bilateral measurements were thereafter combined to give 8 basal ganglia measurements (4 time points each for left and right basal ganglia) for each of the 8 normal control subjects. Linear regression fit errors were never greater than 17% for any single individual brain metabolite.

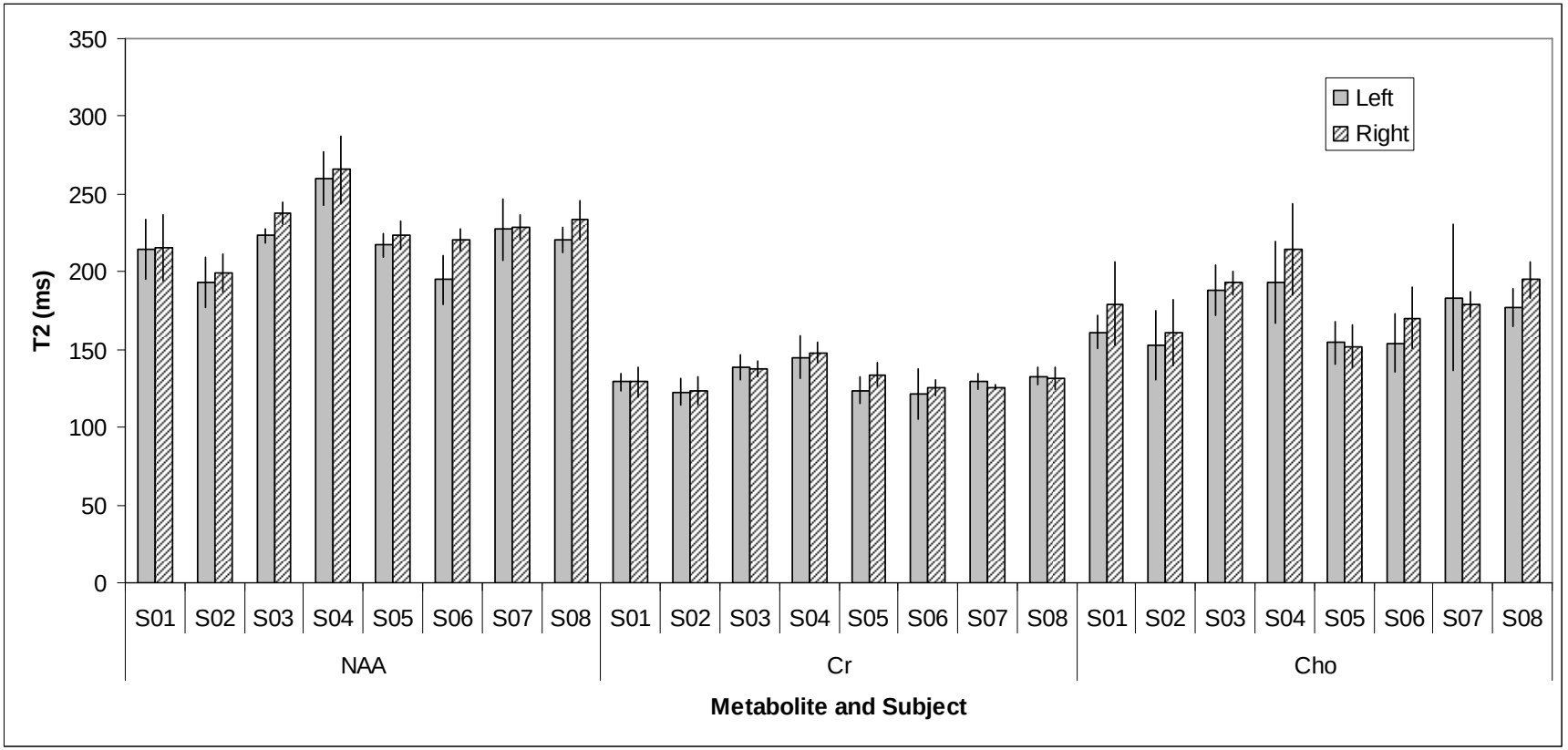

Figure 16: A comparison of T_2 (in ms) in left and right basal ganglia in each control subject, averaged across acquisitions (N=4 for each side).

4.1.1 Intraindividual Variability

The eight sequential (left and right each measured four times) basal ganglia measurements within subjects were used to assess intraindividual variability. Results (mean for each subject) for each metabolite (NAA, Cr_t, and Cho_t) are shown in Table 1. Mean coefficient of variation (CV) values for the eight subjects are 6% (range 4-8%) for NAA, 6% (range 3-9%) for Cr_t, and 11% (range 6-17%) for Cho_t. The eight measurements taken (four each for left and right basal ganglia) in each subject are shown with mean and two standard deviations (± 1 S.D.) in Figure 17 (for NAA), Figure 18 (for Cr_t), and Figure 19 (for Cho_t).

			NAA			Cr			Cho		
AGE/SEX	AVG T_2*	SUBJECT	MEAN	STDEV	CV (%)	MEAN	STDEV	CV (%)	MEAN	STDEV	CV (%)
48/M	31.2	S01	215	19	9%	129	7	6%	170	21	12%
37/M	35.1	S02	196	13	6%	123	8	6%	157	20	13%
47/M	30.8	S03	230	9	4%	138	6	4%	191	12	6%
25/M	29.3	S04	262	18	7%	146	10	7%	204	28	14%
25/F	28.1	S05	220	8	4%	129	9	7%	153	12	8%
38/F	33.5	S06	208	17	8%	123	11	9%	162	20	12%
37/M	32.1	S07	228	14	6%	127	4	3%	181	31	17%
25/M	33.8	S08	227	12	5%	132	6	4%	186	14	7%
		AVG	223	14	6%	131	7	6%	176	20	11%

Table 1. Cerebral metabolite (NAA, Cr_t, and Cho_t) T_2 relaxation data (in ms) for normal control subjects 1-8, including age in years, sex, and average T_2* for acquisitions, as reported for the raw water peak by the Siemens hardware. N=8 for each subject (four measurements each for right and left basal ganglia).

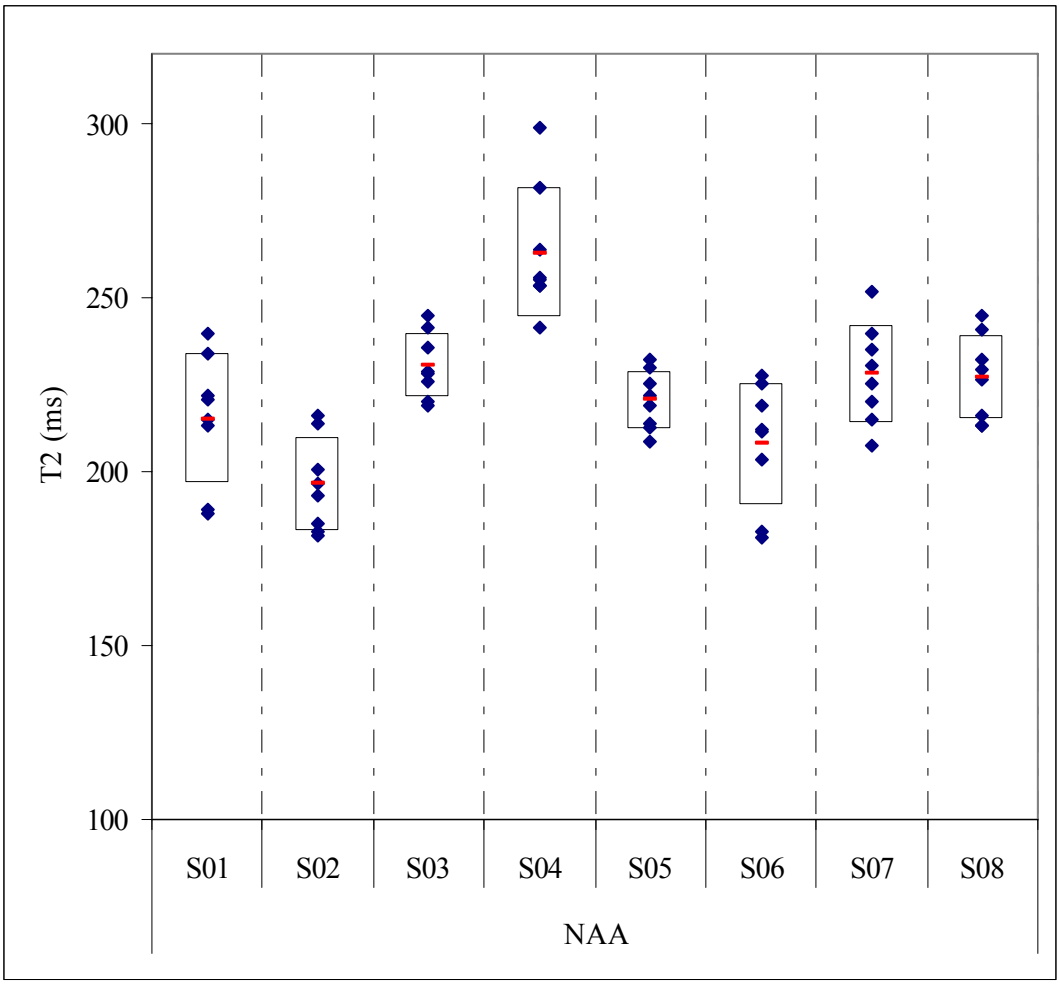

Figure 17. NAA T_2 values for individual normal control subjects. The box represents 2 standard deviations, ± 1 S.D from the mean (represented by horizontal red dash).

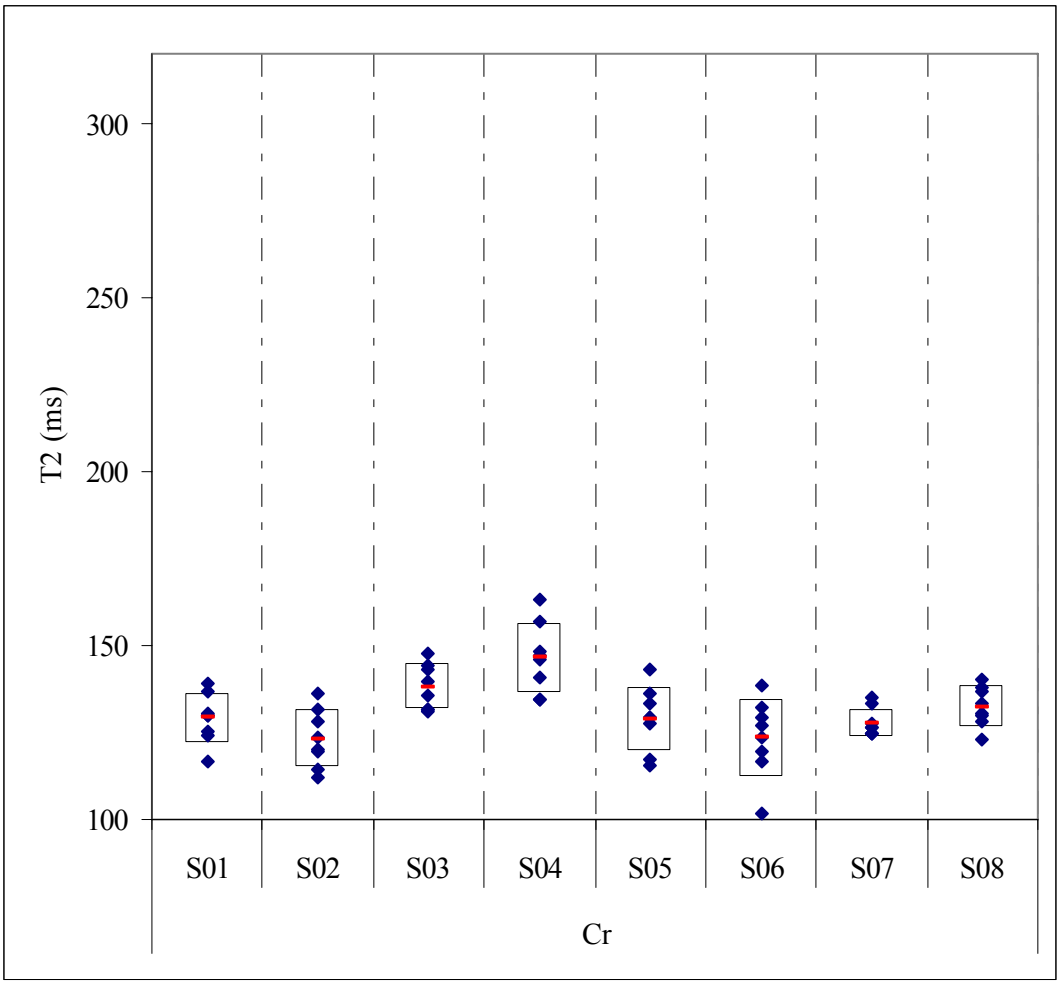

Figure 18. Cr_t T_2 values for individual normal control subjects. The box represents 2 standard deviations, ± 1 S.D from the mean (represented by horizontal red dash).

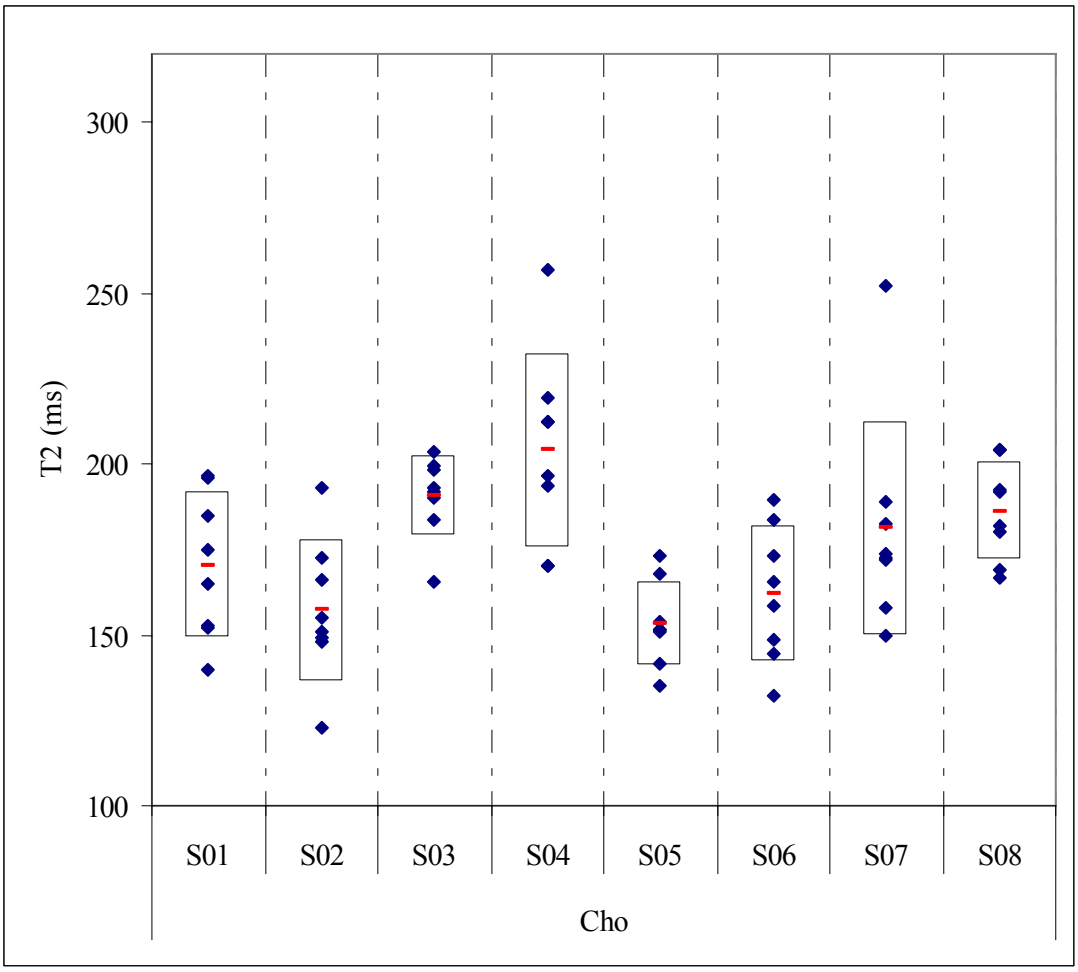

Figure 19. Cho_t T_2 values for individual normal control subjects. The box represents 2 standard deviations, ± 1 S.D from the mean (represented by horizontal red dash).

4.1.2 Interindividual Variability

Interindividual variability was investigated by repeating the same measurement parameters on 8 different normal controls. Though brain sizes among individuals differ, the voxels were appropriately sized (20x30x20mm) to be placed reproducibly and homogeneously within the basal ganglia region for all subjects and sessions. Moreover, the acquisition parameters were chosen to allow sufficient SNR, even at long TE, to obtain usable results for all metabolites, in all subjects and sessions. Coefficients of

variation (CVs) for T_2 of the metabolites are 9% for NAA, 5% for Cr_t, and 10% for Cho_t, between individuals studied.

4.2 T_2 Measurements in GWI Patient Population

Of the 56 subjects that participated in the overall GWI pilot study on CB veterans, 3 subjects withdrew from the study mid-way through data acquisition, 2 subjects were claustrophobic and could not complete the duration of the spectroscopy exam. Of the 106 remaining basal ganglia spectra (both left and right for each subject), all metabolites could be resolved and quantified, though 2 more spectra were eliminated due to high error on the fit of the regression line. The remaining spectra are distributed as follows: in the left basal ganglia, 10 Syndrome 1 subjects, 14 Syndrome 2 subjects, 11 Syndrome 3 subjects, and 14 veteran control subjects; in the right basal ganglia, 11 Syndrome 1 subjects, 17 Syndrome 2 subjects, 11 Syndrome 3 subjects, and 15 veteran controls. All metabolites were resolved and quantified for the 103 remaining basal ganglia data sets. A summary of results is shown in Table 2 through Table 7, and detailed results for individual veterans are shown in Table 8 and Table 9.

	Left Basal Ganglia NAA T_2 Times (ms)			
	Veteran Controls	Syndrome 1	Syndrome 2	Syndrome 3
AVG	194	194	217	206
STD	29	17	19	27
CV(%)	14.67%	8.99%	8.83%	12.95%
N	14	10	14	11

Table 2. NAA T_2 relaxation times (in ms) for left basal ganglia in Gulf War veteran population.

	Right Basal Ganglia NAA T_2 Times (ms)			
	Veteran Controls	Syndrome 1	Syndrome 2	Syndrome 3
AVG	218	217	213	211
STD	19	17	23	20
CV(%)	8.69%	7.83%	10.94%	9.54%
N	15	11	17	11

Table 3. NAA T_2 relaxation times (in ms) for right basal ganglia in Gulf War veteran population.

	Left Basal Ganglia Cr_t T_2 Times (ms)			
	Veteran Controls	Syndrome 1	Syndrome 2	Syndrome 3
AVG	119	119	127	122
STD	11	10	8	13
CV(%)	9.15%	8.6%	6.61%	10.52%
N	14	10	14	11

Table 4. Cr_t T_2 relaxation times (in ms) for left basal ganglia in Gulf War veteran population.

	Right Basal Ganglia Cr_t T_2 Times (ms)			
	Veteran Controls	Syndrome 1	Syndrome 2	Syndrome 3
AVG	131	132	131	125
STD	13	10	15	8
CV(%)	10.2%	7.78%	11.68%	6.37%
N	15	11	17	11

Table 5. Cr_t T_2 relaxation times (in ms) for right basal ganglia in Gulf War veteran population.

	Left Basal Ganglia Cho_t T_2 Times (ms)			
	Veteran Controls	Syndrome 1	Syndrome 2	Syndrome 3
AVG	159	157	167	161
STD	34	18	19	21
CV(%)	21.10%	11.74%	11.15%	13.03%
N	14	10	14	11

Table 6. Cho_t T_2 relaxation times (in ms) for left basal ganglia in Gulf War veteran population.

	Right Basal Ganglia Cho_t T_2 Times (ms)			
	Veteran Controls	Syndrome 1	Syndrome 2	Syndrome 3
AVG	162	162	178	169
STD	16	22	20	13
CV(%)	9.77%	13.58%	11.68%	7.85%
N	15	10	17	11

Table 7. Cho_t T_2 relaxation times (in ms) for right basal ganglia in Gulf War veteran population

				LBG		
Subj#	Synd.	Age	T_2*	**NAA T_2**	**Cr T_2**	**Cho T_2**
4	2	60	24			
5	VC	71	25	**170**	**106**	**122**
6	VC	59	27	**193**	**118**	**158**
7	2	73	29	**250**	**127**	**155**
8	2	71	27			
9	2	58	27	**244**	**137**	**136**
10	2	65	27	**186**	**127**	**152**
11	VC	61	28	**230**	**117**	**186**
12	2	60	30	**241**	**124**	**173**
13	2	61	28	**209**	**130**	**168**
14	VC	51	28	**212**	**127**	**172**
15	VC	66	27	**231**	**129**	**162**
16	2	54	29	**221**	**110**	**158**
17	VC	76	30			
18	2	70	33	**225**	**136**	**199**
19	VC	64	32	**211**	**137**	**175**
21	3	61	26	**208**	**110**	**147**
22	1	60	28	**196**	**108**	**183**
23	VC	58	22	**132**	**103**	**106**
24	3	60	27	**211**	**110**	**130**
25	2	53	26	**225**	**128**	**153**
26	1	49	31	**215**	**120**	**165**
27	1	53	28	**205**	**129**	**167**
28	VC	59	24	**180**	**115**	**132**
29	VC	63	31	**183**	**112**	**164**
30	VC	52	28	**201**	**131**	**151**

31	2	61	26	**247**	**147**	**211**
32	2	57	32	**188**	**134**	**163**
33	3	61	30	**169**	**113**	**130**
34	1	52	28	**207**	**120**	**167**
35	VC	56	27	**155**	**103**	**134**
36	VC	61	31	**216**	**130**	**200**
37	2	69	27	**216**	**135**	**182**
38	3	47	31	**203**	**139**	**175**
39	1	44	28	**195**	**139**	**169**
40	3	59	24	**181**	**119**	**172**
41	VC	55	31	**190**	**121**	**136**
42	3	60	31	**168**	**108**	**149**
43	3	50	29	**222**	**133**	**157**
44	2		26	**210**	**131**	**199**
45	1		26	**214**	**114**	**144**
46	1	47	26	**171**	**119**	**136**
47	3	66	27	**192**	**115**	**178**
48	3		30	**250**	**126**	**196**
49	VC	61	27	**216**	**116**	**234**
50	1	52	27	**196**	**123**	**170**
51	3	50	27			
52	3	63	26	**239**	**145**	**176**
53	1	53	28	**288**	**154**	**241**
54	1	59	27	**180**	**119**	**137**
55	1	56	28	**164**	**102**	**129**
56	3	47	25	**220**	**129**	**160**
57	2	63	26	**217**	**124**	**179**
58	VC	69	35			
59	2	56	25	**214**	**118**	**174**
60	2	66	26	**198**	**113**	**149**
AVG		59.02	27.84	205.98	123.22	163.95
STD		7.20	2.48	27.78	11.96	26.82
CV%		**12.20%**	**8.90%**	**13.49%**	**9.70%**	**16.36%**

Table 8. Left basal ganglia data for individual gulf war veteran subjects, including fit errors, group membership, raw water T_2* values as reported by the hardware, and ages (in years) for each subject. VC = Veteran Controls; all subjects were male.

				RBG		
Subj#	Synd.	Age	T_2*	**NAA T_2**	**Cr T_2**	**Cho T_2**
4	2	60	26	**242**	**131**	**185**
5	VC	71	30			
6	VC	59	24	**221**	**127**	**142**
7	2	73	35	**225**	**134**	**169**
8	2	71	25	**166**	**107**	**168**
9	2	58	29	**226**	**163**	**138**
10	2	65	25	**185**	**110**	**156**
11	VC	61	30	**238**	**136**	**171**
12	2	60	28	**222**	**148**	**181**
13	2	61	28	**187**	**121**	**161**
14	VC	51	30	**232**	**124**	**135**
15	VC	66	27	**234**	**137**	**180**
16	2	54	29	**251**	**153**	**193**
17	VC	76	27	**243**	**154**	**159**
18	2	70	32	**219**	**143**	**211**
19	VC	64	31	**235**	**155**	**171**
21	3	61	28	**215**	**128**	**156**
22	1	60	30	**230**	**147**	**119**
23	VC	58	23	**230**	**106**	**160**
24	3	60	26	**227**	**132**	**191**
25	2	53	27	**219**	**130**	**194**
26	1	49	31	**227**	**120**	**178**
27	1	53	27	**226**	**134**	**176**
28	VC	59	26	**184**	**123**	**161**
29	VC	63	28	**203**	**124**	**182**
30	VC	52	26	**213**	**133**	**167**
31	2	61	27	**238**	**125**	**166**
32	2	57	32	**182**	**118**	**162**
33	3	61	25	**194**	**126**	**169**
34	1	52	29	**219**	**145**	**243**
35	VC	56	24	**178**	**115**	**140**
36	VC	61	30	**216**	**137**	**148**
37	2	69	29	**216**	**124**	**178**
38	3	47	30	**229**	**125**	**181**
39	1	44	34	**229**	**125**	**181**
40	3	59	27	**193**	**119**	**144**
41	VC	55	32	**210**	**128**	**168**
42	3	60	30	**190**	**115**	**165**
43	3	50	29	**179**	**112**	**168**
44	2		26	**202**	**133**	**217**
45	1		26	**185**	**125**	**143**
46	1	47	29	**215**	**127**	**135**
47	3	66	29	**231**	**131**	**163**
48	3		31	**231**	**120**	**185**
49	VC	61	27	**219**	**121**	**156**

50	1	52	29	**236**	**127**	**174**
51	3	50	29			
52	3	63	30	**231**	**134**	**169**
53	1	53	27	**225**	**147**	**175**
54	1	59	28	**199**	**135**	**178**
55	1	56	26	**193**	**121**	**158**
56	3	47	26	**198**	**136**	**165**
57	2	63	32	**232**	**141**	**195**
58	VC	69	32	**209**	**140**	**189**
59	2	56	26	**199**	**135**	**178**
60	2	66	28	**208**	**113**	**168**
AVG		59.02	28.34	214.55	130.03	169.72
STD		7.20	2.54	19.91	12.49	21.36
CV%		**12.20%**	**8.96%**	**9.28%**	**9.60%**	**12.59%**

Table 9. Right basal ganglia data for individual gulf war veteran subjects, including fit errors, group membership, raw water T_2* values as reported by the hardware, and ages (in years) for each subject. VC = Veteran Controls; all subjects were male.

Average values of T_2 for all three metabolites in both hemispheres were significantly lower for veteran control subjects (59±7.2 years) than for the younger normal controls (37.5±10.9 years) or literature values; for example, average NAA T_2 in both basal ganglia of 206 ms in veteran control subjects compared to 223 ms in non-veteran normal controls. However, there is literature that suggests that T_2 times decrease with age – a 15% reduced T_2 in NAA of elderly subjects (74±3 years old) as compared to young adults (26±1 years) was shown in the putamen region, along with a 16% reduction in Cr_t T_2 times and a 5% reduction in Cho_t T_2 times (Kirov, Fleysher et al. 2008). T_2 values versus age in years for both normal controls and veteran controls of this study are shown in Figure 20, with trend lines plotted for normal control subjects, showing a non-significant trend which reflects a similar decrease in T_2 times with age as described in literature, however, this cannot be made significant with the few subjects presented here. A similar plot of T_2 relaxation times versus age in years in Figure 21 shows no evidence of such a trend in ill Gulf War veterans. Because the veteran population was about 21.5

years older, on average (as summarized in Figure 22), than the younger normal controls in the reproducibility study, the shorter T_2 relaxation times observed in the veteran controls may be attributed in large part to an age effect - however, the data available in this study does not represent a sufficient age spectrum to recreate Kirov's conclusion.

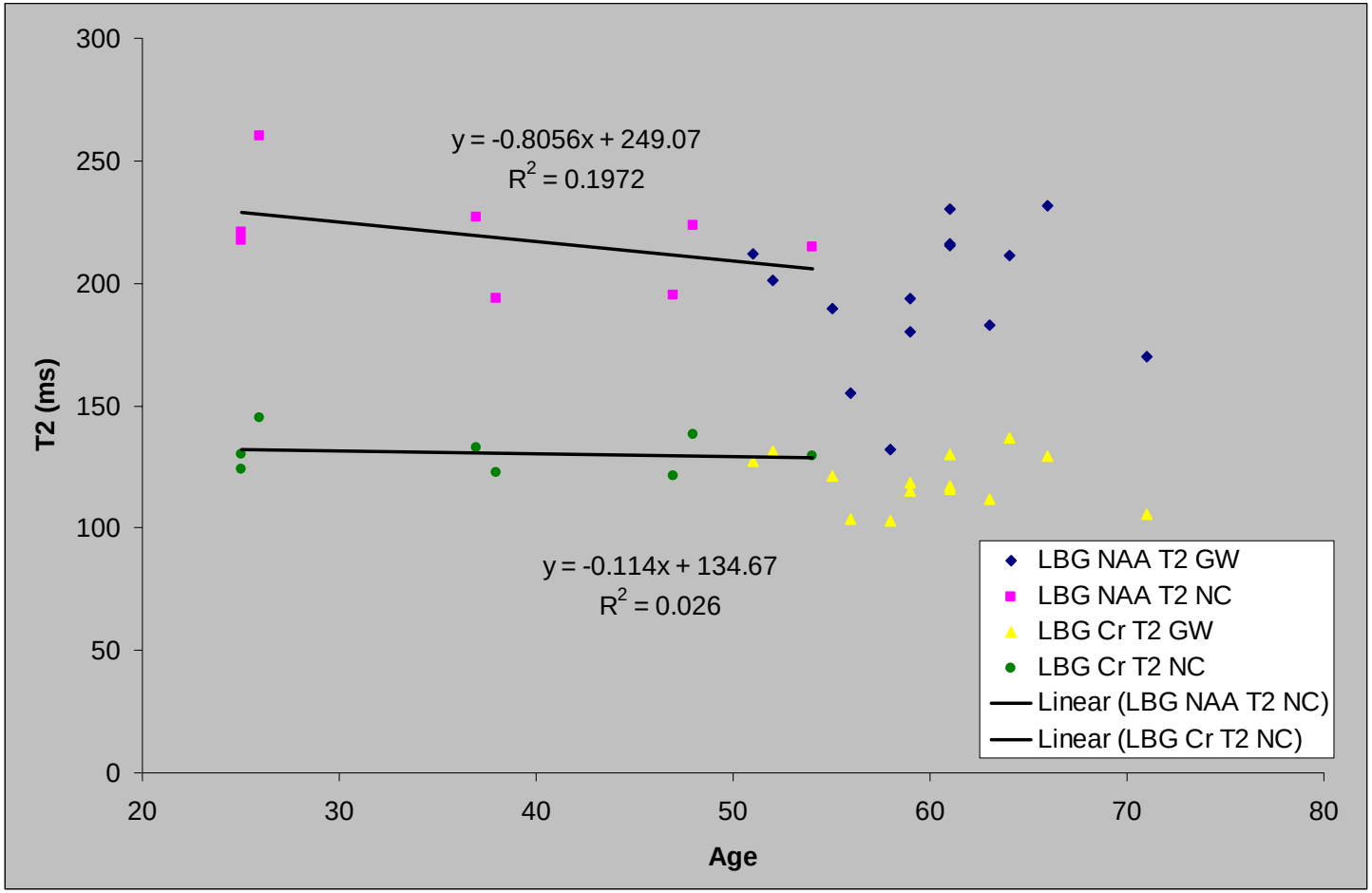

Figure 20. Transverse relaxation times (in ms) of normal and veteran controls for NAA and Cr_t metabolites plotted versus age (in years) of individual subjects, with trend lines applied to normal control subject data.

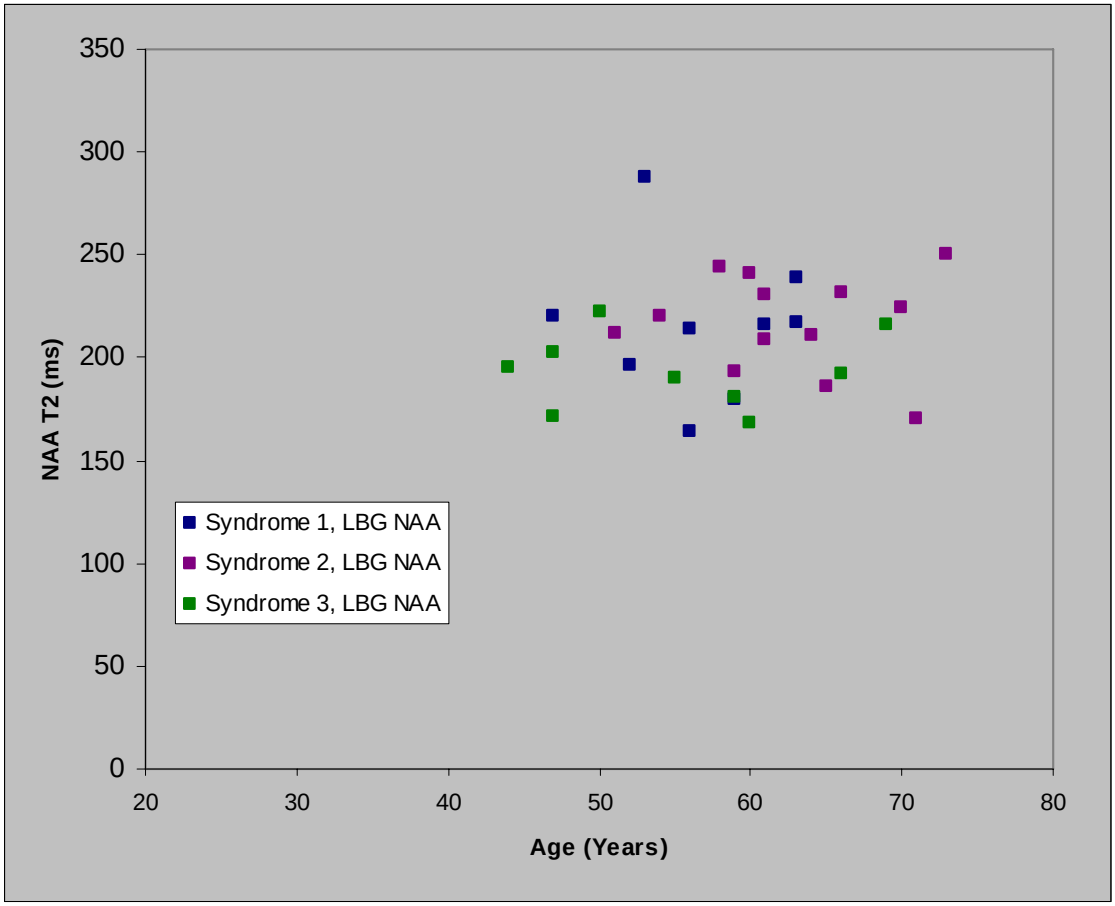

Figure 21. Transverse relaxation times (in ms) of ill Gulf War Veterans in left basal ganglia NAA plotted versus age (in years) for individual subjects.

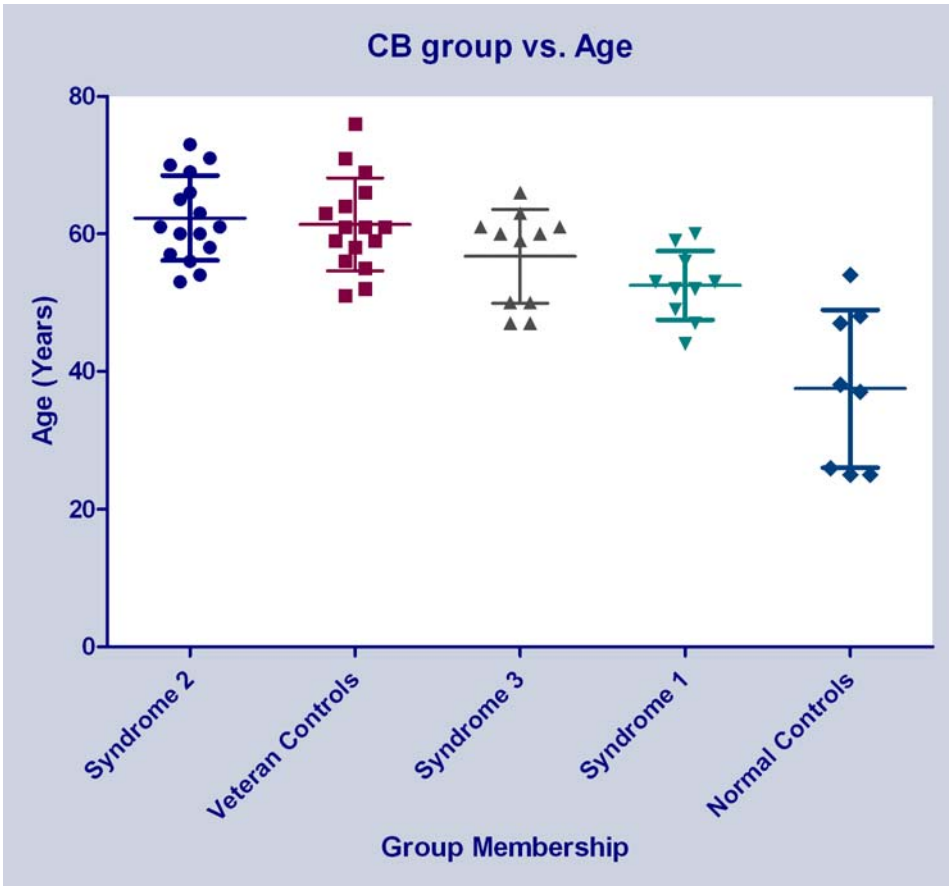

Figure 22. Age demographic data by group membership, shown with bars ±1 S.D.

4.2.1 Metabolite Transverse Relaxation Variation Hypothesis

Hypothesis 2 stated that GWI veterans would exhibit different basal ganglia metabolite T_2 values than veteran control subjects, and that Syndrome 2 subjects were expected to show the largest difference in relaxation time from controls of the three major Gulf War syndromes. Within the veteran population, significant ($p<0.05$) differences were observed between the Syndrome 2 patient population and the veteran controls in left basal ganglia NAA T_2 (11.4% longer for Syndrome 2, $p=0.019$) and Cr_t T_2 (6.4% longer in Syndrome 2, $p=0.044$), and right basal ganglia Cho_t T_2 (9.55% longer in Syndrome 2,

p=0.021). There are significant differences in NAA T_2 between syndrome classifications 2 and 1 (11.35% longer in Syndrome 2 than Syndrome 1, p=0.007), however, Syndrome 1 T_2 data closely mirrors normal veteran control T_2 data in both mean and distribution. Data are shown graphically in Figure 23, Figure 24, and Figure 25.

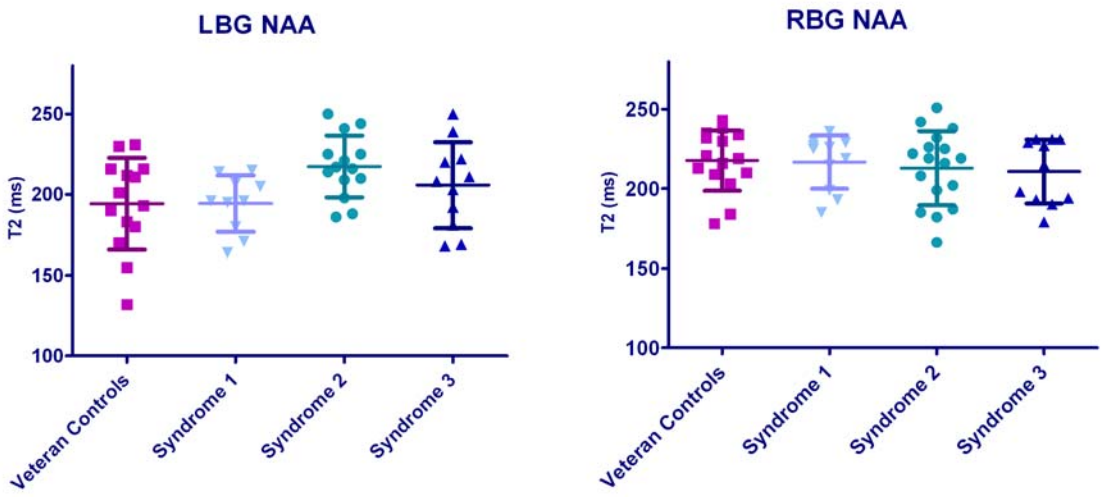

Figure 23. Left and right basal ganglia NAA T_2 relaxation times (in ms) for Gulf War veteran subjects

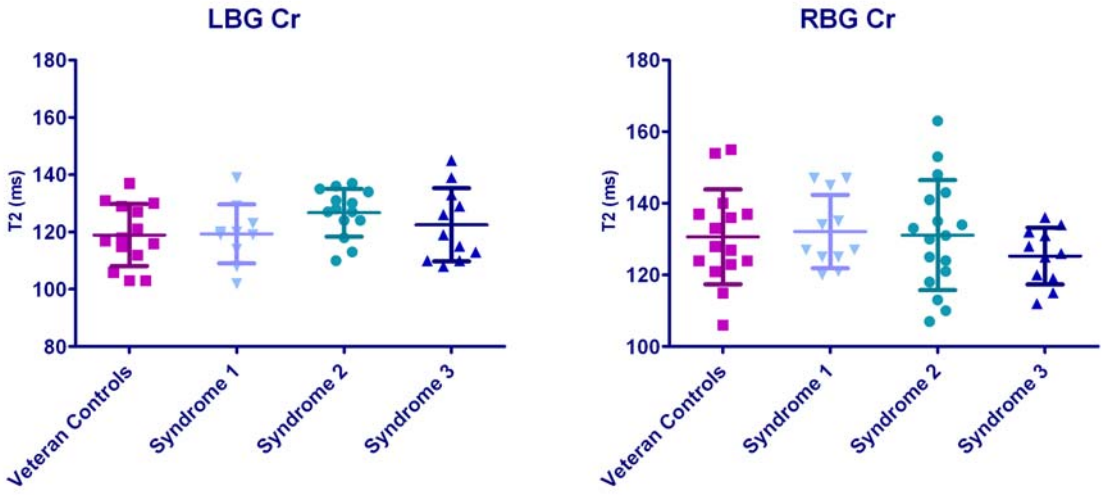

Figure 24. Left and right basal ganglia Cr_t T_2 relaxation times (in ms) for Gulf War veteran subjects

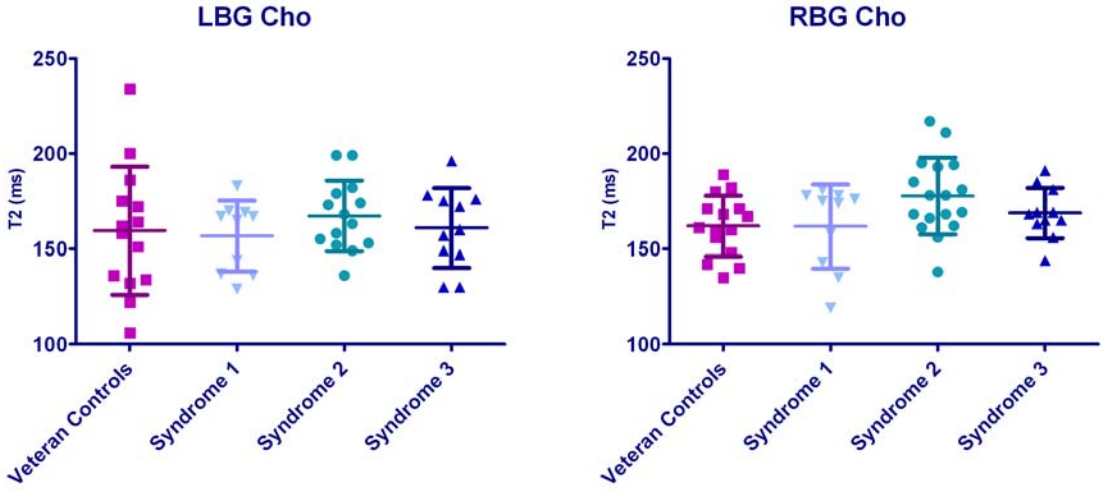

Figure 25. Left and right basal ganglia Cho_t T_2 relaxation times (in ms) for Gulf War veteran subjects

4.2.2 Concentration Effect Hypothesis

Because one goal of the study was to verify findings from the 1998 Haley study, which used TE=272 ms, T_2 relaxation was obtained with the intention of correcting metabolite concentration calculations, to move toward absolute quantitation. Specifically, the aim of the concentration effect hypothesis was to correct metabolite signal intensities (analyzed by other members of the MRS sub-core) with the measured T_2 relaxation times to assess the degree to which differences in T_2 contribute to signal intensity differences, and to compare relaxation-corrected values.

One approach to this concept of correction is to correct metabolite concentration values or ratios of individual subjects in groups with the T_2 group average, shown to be significantly different between certain metabolites and groups (see above). However, even for the statistically significant difference in T_2 relaxation times between Syndrome 2 veterans and veteran controls, the resulting correction factors are very nearly the same for the four groups, differing by approximately 1% or less (as shown in Table 10), indicating that the group differences for the left and right basal ganglia NAA/Cr_t ratio measured at TE=30 ms, after applying correction factors, are very small, and even smaller for Cho_t/Cr_t ratio group differences, since the groups have smaller differences in T_2 for Cr_t and Cho_t than for NAA, as discussed above.

	Correction Factors for NAA/Cr_t Concentration Data in Basal Ganglia			
	Veteran Controls	Syndrome 1	Syndrome 2	Syndrome 3
Left	1.102	1.102	1.103	1.105
Right	1.096	1.093	1.092	1.103

Table 10. Concentration correction factors in right and left basal ganglia for NAA/Cr_t ratio calculations, measured at TE=30 ms.

The second approach to correction is to correct each individual subject's data with his own measured T_2 value for each metabolite. The drawback to this method is additional loss of data due to either set of data being compromised in any way. In this case, one additional subject (Syndrome 1 group) was lost during the TE=30 ms concentration analysis. Results of this analysis are shown in Figure 26 and Figure 27. Though means for each group have increased by approximately 10% for each classification group for the NAA/Cr_t results and approximately 5% for each classification group for the Cho_t/Cr_t, standard deviations and significances remain largely unchanged across the board. This result, however, was derived from concentration values taken at TE=30 ms, when relaxation effects are at a minimum, so a relatively small change in concentration values is not unexpected.

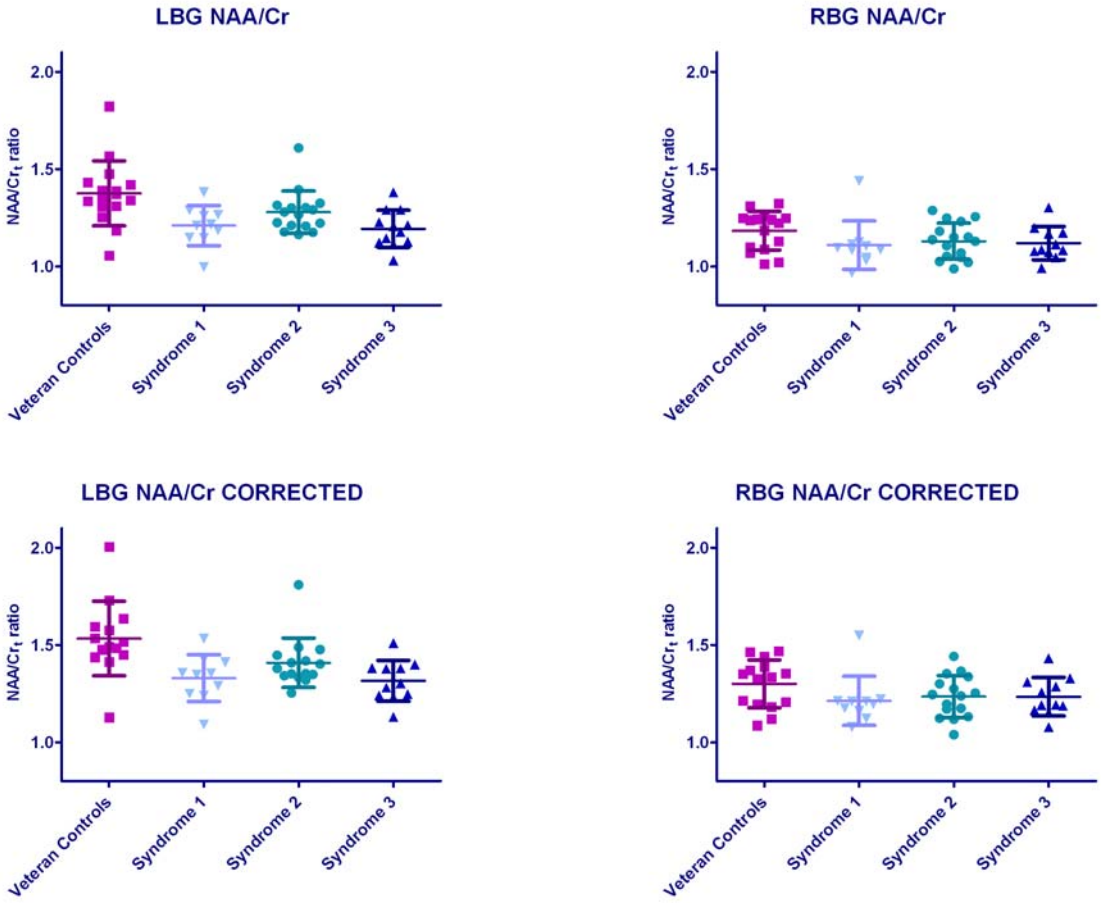

Figure 26. NAA/Cr$_t$ concentration ratios in left and right basal ganglia from TE=30 ms data (as obtained by Dr. Sergey Cheshkov of the MRS sub-core), uncorrected and corrected with individual T_2 values.

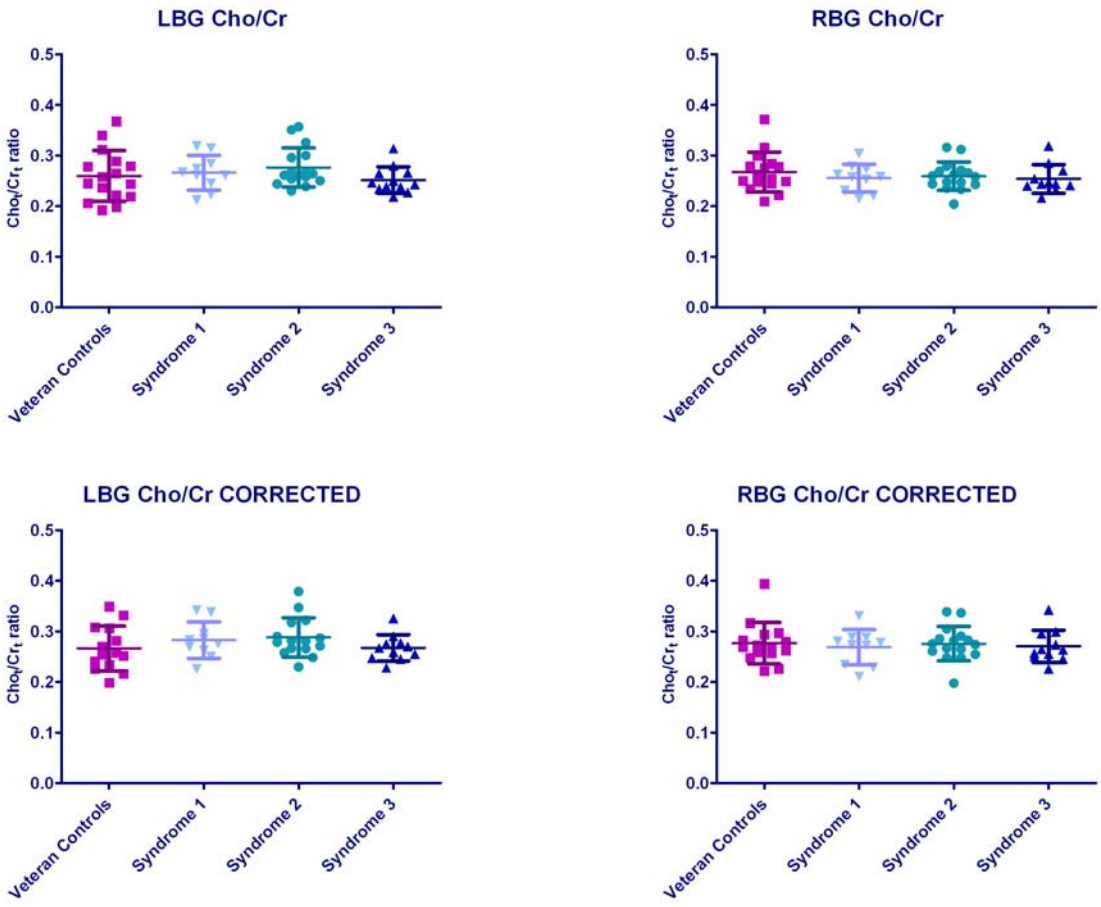

Figure 27. Cho_t/Cr_t concentration ratios in left and right basal ganglia from TE=30 ms data (as obtained by Dr. Sergey Cheshkov of the MRS sub-core), uncorrected and corrected with individual T_2 values.

The TE=270 ms concentration data (analyzed by Dr. Hyeonman Baek of the MRS sub-core) showed NAA concentration differences between Syndrome 2 and veteran controls, however these data exhibited a high distribution of values and an even greater loss of subject numbers (12 remaining left basal ganglia data sets each for Syndrome 2 subjects and veteran controls subjects for analysis), largely attributed to lower signal to noise ratio at long TE times, and did not reach accepted levels of significance ($p>0.05$). Shown in Figure 28 and Figure 29 are the concentration values for Syndrome 2 and

veteran control subjects, corrected and uncorrected for individual T_2 values. Means and standard deviation within groups changed (from uncorrected to corrected values) from 4.37±1.7 mM to 5.9±1.0 mM in Syndrome 2 subjects, and from 5.1±1.8 mM to 6.7±1.6 mM in veteran control subjects. Moreover, several subjects presenting as outliers in uncorrected data were corrected to values within one standard deviation of mean. In addition, differences between Syndrome 2 and veteran controls improved (from p=0.13 to p=0.08), if not quite reaching the significance threshold value of p=0.05.

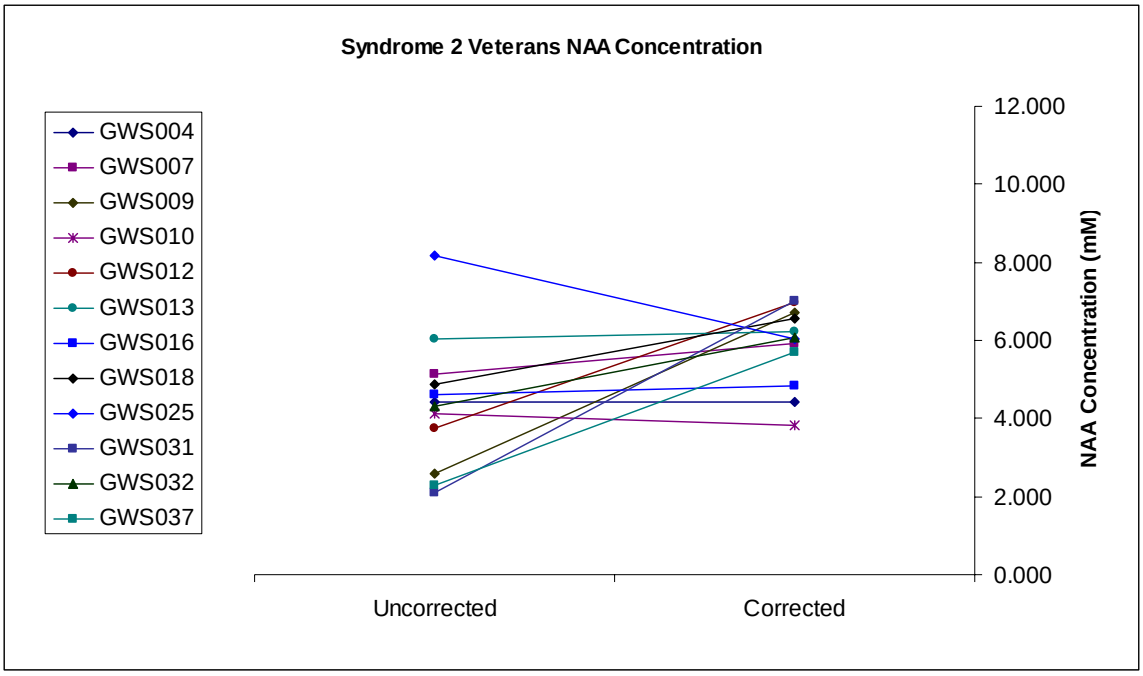

Figure 28. NAA concentration values in left basal ganglia of Syndrome 2 veterans from TE=270 ms data (as obtained by Dr. Hyeonman Baek of the MRS sub-core), corrected and uncorrected for individual T_2 values.

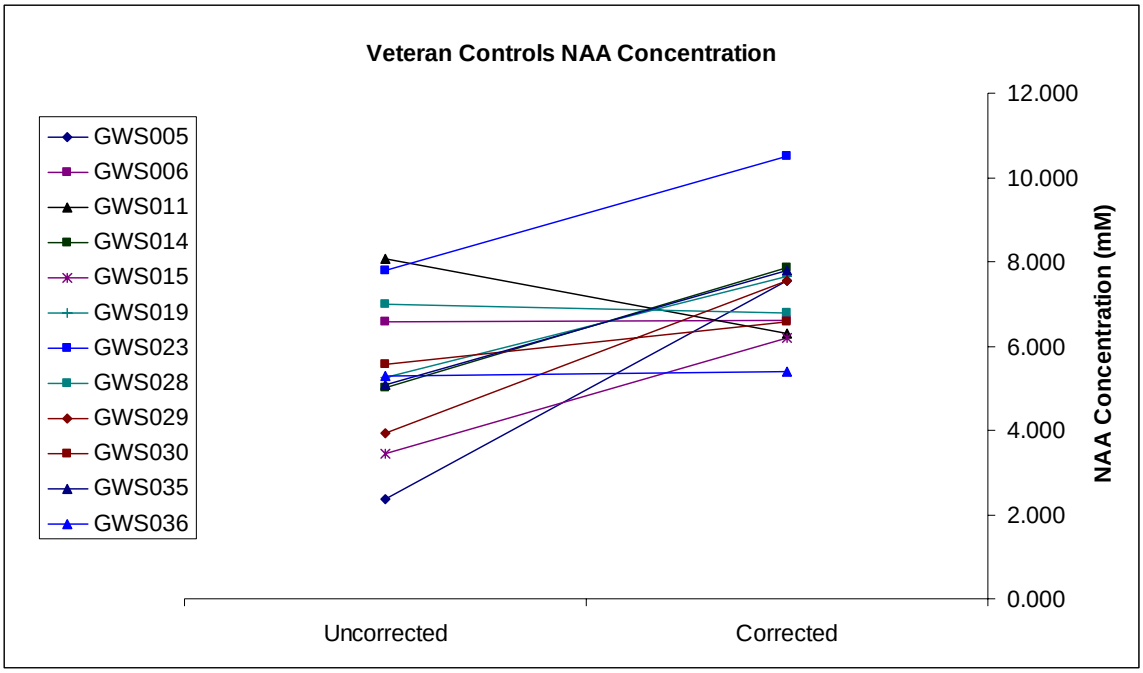

Figure 29. NAA concentration values in left basal ganglia of normal veteran control subjects from TE=270 ms data (as obtained by Dr. Hyeonman Baek of the MRS sub-core), corrected and uncorrected for individual T_2 values.

5 DISCUSSION

Relaxation times have long been an assumed value in spectroscopy studies, and have had limited usage in studies of disease or progressive disorders. The purpose of this study was to develop and apply protocols to measure the transverse (T_2) relaxation times of the major brain metabolites (NAA, Cr_t, and Cho_t) to determine if the T_2 values differ between veterans with Gulf War Illness (GWI) and age-matched normal controls, and to investigate if T_2 relaxation values differ amongst the Haley-defined syndrome classifications.

5.1 Normal Control Reproducibility Study

The first step in this study of transverse relaxation time was to reliably ascertain whether T_2 measurements with adequate precision and reproducibility could be made using the current equipment and limited scan times to be useful in studies involving the basal ganglia and subtle changes due to axonal damage or loss. This aim was achieved for relaxation measurements in the studied region.

Previous studies on the inter-subject measures of variability of T_2 relaxation data have not established reproducibility in more than two subjects over time (Mlynarik, Gruber et al. 2001; Traber, Block et al. 2004; Zaaraoui, Fleysher et al. 2007) , and other studies on reproducibility and quantification of metabolites in proton MR spectroscopy (Li, Babb et al. 2002; Hammen, Stadlbauer et al. 2005) do not take into account the

potential T_2 relaxation times to be affected by progressive diseases. Zaaraoui et al. (Zaaraoui, Fleysher et al. 2007) performed T_2 relaxation measurements at 3T using chemical-shift imaging with approximately 1 cm^3 voxel resolution in a 2D 16x16x4 cm^3 slice in under 70 minutes. However, by utilizing only two TE data points, the quality of the line fit cannot be established. Also, individual voxel shims will not be homogeneous over such a large area without readjustment – there is no dependable way to account for the possible error in the measurement due to magnet inhomogeneity. There are several advantages to using single voxels for areas of interest, instead of manually-drawn ROIs and 1 cm^3 voxels chosen after acquisition: more accurate spatial localization can be made to the anatomy of interest, adjustments can be made for anatomical variations in individual subjects, and manual shimming can be performed on each individual voxel for greater reproducibility and accuracy. Zaaraoui's methods, and similar studies, cannot produce the accuracy or robust reliability required by this study. The only comparable study of T_2 relaxation in specific brain regions was performed by Traber et al. (Traber, Block et al. 2004), who established T_2 values for brain metabolites in the basal ganglia which are significantly lower than values in other investigated brain regions (NAA T_2 = 221±18 ms (± SD), Cr_t T_2 =143±13 ms, Cho_t T_2 = 201±16 ms, group average, N=8). The group average of the eight normal controls in this reproducibility study was in good agreement for NAA (T_2 = 223±13 ms (±SD)), though the averages for Cr_t (T_2 = 131±7 ms) and Cho_t (T_2 = 176±19 ms) are slightly lower than the Traber results. This cannot be attributed to the same age dependence cited earlier, as the age range for the particular volunteers used in the basal ganglia section of the Traber data is not specified. There are also possible variations due to the different voxel sizes (3x2.5x2 cm^3 in Traber, 2x3x2

cm^3 in this study) or voxel positioning, as well as different hardware used (Gyroscan Intera 3T Philips in Traber, Siemens TIM Trio 3T system in this study), and a higher number of signal averages used in this study for higher TE spectra.

One important feature to note is the similar low coefficients of variation (11% or less for all metabolites) in both studies. Results from the reproducibility study in normal controls, shown in Table 1, as well as Figure 17, Figure 18, and Figure 19, demonstrate good reproducibility, both intersubject and intrasubject. This is best demonstrated in the NAA values shown in Figure 17. While subjects have mean values that are significantly different from other subjects, these values are reliably reproduced within each subject. This implies that a single T_2 measurement, taken in under 30 minutes of scan time, reliably estimates the T_2 value of the three major metabolites (NAA, Cr_t, and Cho_t) in basal ganglia at 3T for each individual subject. A T_2 variation of 11%, the maximum measured mean coefficient of variation, would result in a 4% change in estimated metabolite concentration, as described in Equation 1-4.

With the level of reproducibility characterized in this study, the results of the study of veterans with GWI, for which the data were acquired over the period of one year in approximately 60 subjects on the same hardware under the same protocol specifications, could now be interpreted with more assurance.

5.2 Gulf War Illness Patient Study

The second goal of this study was to investigate veterans suffering from Gulf War Illness, specifically to detect changes in basal ganglia NAA, Cr_t, and Cho_t T_2 values as compared to control subjects.

Again, an important feature to note in the data is the lack of exclusion of spectra due to poor metabolite resolution, and the low coefficients of variation (average of 11% for NAA, 9% for Cr_t, and 14% for Cr_t across all subjects in both left and right basal ganglia). This is not only in good agreement with, though slightly more variable than, the earlier reproducibility study, but a very positive result for the age range under study (veteran controls were all male, 44-76 years old, mean age 59±7.2 years), notorious for age-related difficulties in the magnet, including, in this study, one subject who was diagnosed as pre-parkinsonian, another who required an oxygen line, and several others who were unable to remain motionless for extended periods of time. That only three spectra of 106 were rejected due to poor quality of line fit is very encouraging for future tests of this demographic. As for subjects with confounding psychiatric complaints (i.e. depression, post-traumatic stress disorder, anxiety disorder), when compared as a group against the veterans without added diagnoses there was no significant difference in metabolite T_2 values (as shown in Figure 30, Figure 31, and Figure 32), though there was a noticeable trend for subjects with psychiatric complaints to have lower NAA and Cho_t T_2 values in left basal ganglia ($p=0.2$ and 0.14, respectively).

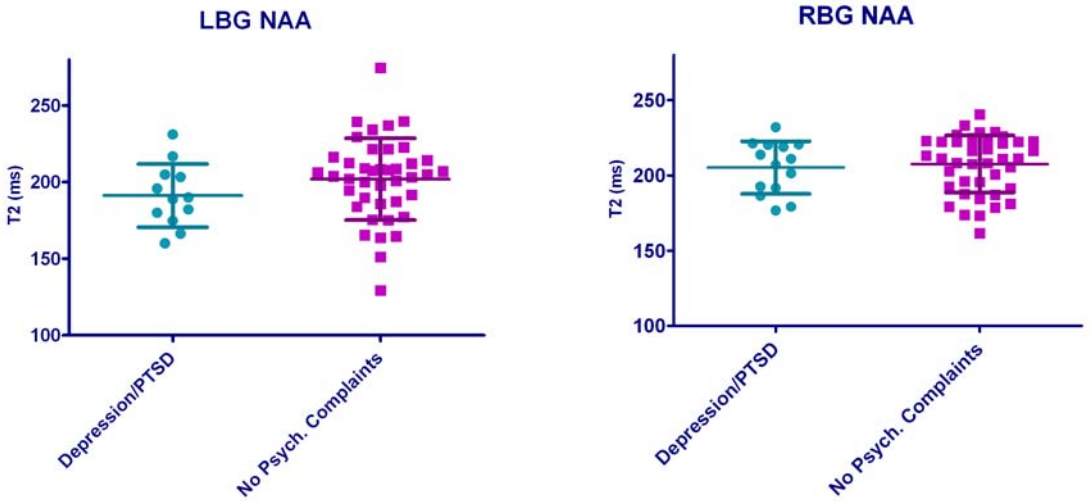

Figure 30. Left and right basal ganglia NAA T_2 relaxation times comparing Gulf War veterans with and without major psychiatric complaints. Psychiatric data tabulation courtesy of Don Aultman.

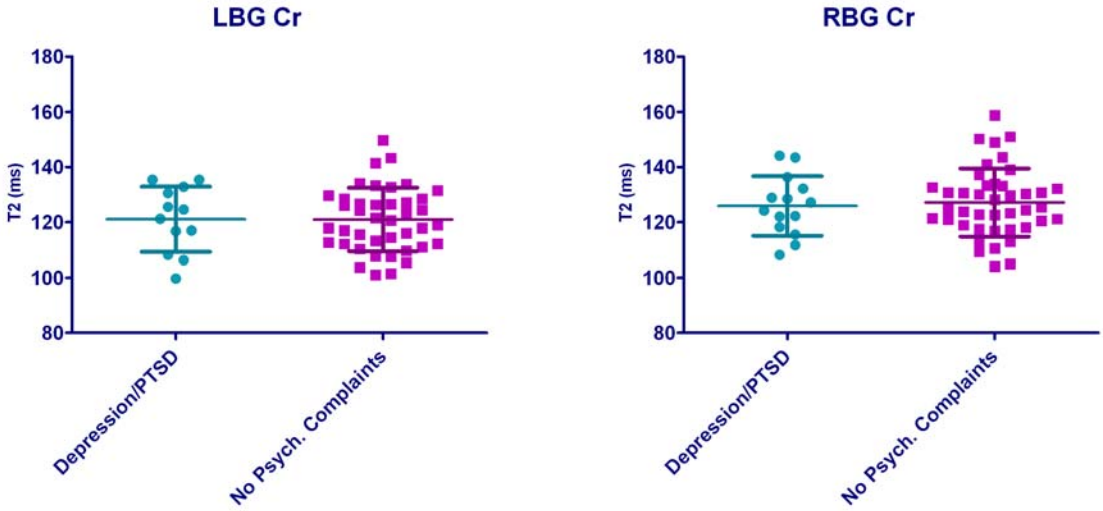

Figure 31. Left and right basal ganglia Cr_t T_2 relaxation times comparing Gulf War veterans with and without major psychiatric complaints.

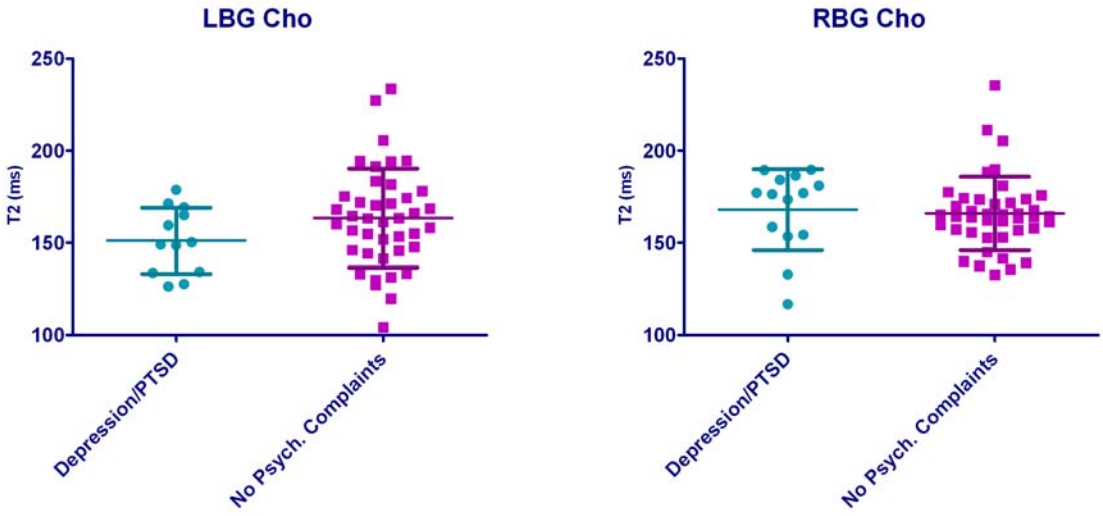

Figure 32. Left and right basal ganglia Cho_t T_2 relaxation times comparing Gulf War veterans with and without major psychiatric complaints. Psychiatric data tabulation courtesy of Don Aultman.

5.2.1 Metabolite Transverse Relaxation Variation Hypothesis

As can be seen from Figure 23, Figure 24, and Figure 25, there are in some cases a significant difference in means of T_2 in the basal ganglia (NAA and Cr_t in left basal ganglia, Cho_t in right basal ganglia in Syndrome 2 subjects as compared to normal controls). However, this difference is only significant in group average, and cannot be concluded to be significant on an individual basis, and thus this information alone is not able to define a single patient as belonging to a specific syndrome classification of GWI.

Previous studies utilizing T_2 relaxation times in a clinical manner include significant changes reported for diseases, such as a reduced T_2 relaxation time in NAA of subjects with Parkinson's disease (Antonini, Leenders et al. 1993) and schizophrenia (Tunc-Skarka, Weber-Fahr et al. 2009) as compared to normal controls. In the case of multiple sclerosis, reduced T_2 relaxation time of NAA was observed not only in voxels

containing brain lesions, but also in white matter that appeared normal on conventional MRI (Schubert, Seifert et al. 2002). A study on relaxation time in metabolites in autism spectrum disorder found lengthened T_2 of Cho in the gray matter of ill versus healthy controls (Petropoulos, Friedman et al. 2006). A trend towards longer T_2 of NAA was found in Alzheimer's patients, but never reached significance due to a large coefficient of variation (Christiansen, Schlosser et al. 1995). A significant increase in T_2 of NAA was observed in HIV seropositive patients with abnormalities in their MRS images, and a non-significant trend towards increased T_2 of NAA was observed in HIV seropositive patients who appeared normal on MRI (Wilkinson, Paley et al. 1994). Increases in all metabolite T_2 relaxation times were observed in infants with poor prognosis in post-natal hypoxic-ischemic injury (Cady 1996; Cheong, Cady et al. 2006) as compared to control infants.

In all these studies, the effect of T_2 relaxation time on concentration and concentration ratio calculations is emphasized, but metabolic reasons for changes in T_2 are often unknown or generalized as microstructural changes (See Appendix). We may hypothesize that increases in metabolite T_2 values may be the observed result of decreased cellular ATP levels and subsequent failure of the sodium-potassium pump, which would cause increased water in cells, creating increased molecular mobility, or any similar manner of cellular water influx. Because one possible theory of physiological damage in the brains of veterans afflicted with Gulf War Illness is neuroinflammation due to organophosphate damage, this could be a very important observation moving forward in the overall GWI study.

Another possible molecular mechanism for metabolite transverse relaxation is chemical exchange (Farrar and Becker 1971; Harris 1986), where a spin can experience a change in molecular environment or configuration. This mechanism can be relevant for enzyme-mediated metabolite reactions *in vivo* or for binding of small metabolite molecules to large molecules, depending on chemical exchange rates between molecular states.

The present study provides a compelling argument to investigate T_2 relaxation in metabolites, not just for concentration calculation correction, but for determination of disease states when conventional MRI shows no abnormalities.

5.2.2 Concentration Effect Hypothesis

The final goal of this study was to explore the potential effect of transverse relaxation time measured *in vivo* on the concentration determination in the same brain areas for the same investigated metabolites. As established earlier, the method determined to have greatest effect on metabolite concentration values is to individually correct each subject with his own measured relaxation time values. Also, as predicted in Equation 1-4, concentration values obtained at low TE (TE=30 ms in this study) are minimally affected by T_2 relaxation correction (a uniform increase of approximately 10% for each groups in this study). This result emphasizes the concentration results, increasing confidence that significant differences observed between syndrome classifications and veteran controls are truly the result of biochemical changes instead of T_2 relaxation changes.

As for this and other studies done at long TE (TE=270 ms in this study), the results shown here strongly support T_2 relaxation correction for long TE acquisitions. Not only are standard deviation distributions improved, but also, subjects that may present as outliers in uncorrected data were shown in this study to be corrected to within one standard deviation of mean. Without T_2 correction in this case, some subjects would have been mislabeled as outliers. Also, with narrower distributions, significant differences are more easily observed.

5.3 Limitations

As discussed earlier, potential movement during the scans cannot be corrected in post-processing on the current hardware. Some patients exhibited difficulty remaining motionless in the scanner for extended periods of time due to chronic back or neck pain, bladder or prostate problems, or, in one case, pre-parkinsonian disorder. Though slight movements could potentially be shifting the selected voxel during acquisition and averaging, the resultant baseline was never disturbed to a significant or observable level. Acquiring data in smaller blocks and aligning the frequency axes using NAA as a common reference could reduce frequency shifts caused by motion.

Actual, as opposed to apparent, transverse relaxation times could also be underestimated by not accounting for diffusion effects causing signal decay. Because diffusion is based upon the random movements of nuclei during TE, the signal reduction is more pronounced at higher TE, and dependent on magnetic field gradients (G) and the

diffusion coefficient ($\mathscr{D}$). A technique for quantifying the effect of diffusion is discussed in Appendix A, but was not applied in this study. Because the direction and magnitude of these corrections should be similar for all groups, they are not expected to significantly alter group comparisons in relaxation data, biomarker applications, or group correction data. However, for the purpose of investigating molecular mechanisms of disease effects on relaxation times, use of uncorrected T_2 data could lead to inaccurate conclusions.

Another possible source of error may be introduced by modeling the spectra in jMRUI for only three peaks and fitting via a linear regression instead of an exponential regression. These slight changes to post-processing protocol should be investigated in future iterations of this study.

Another limitation of this study was that the ill and healthy veterans were not chosen at random from the population. They were pre-selected by Dr. Haley based on the results of a survey distributed in the early 1990s concerning their involvement in the Persian Gulf War and their GWI symptoms. They were all from the same construction brigade (the Twenty-fourth Reserve Naval Mobile Construction Battalion), and supposedly are a representative cross-section of the larger Gulf War veteran population, except for a relatively higher prevalence of post-war illness (Haley, Hom et al. 1997). However, this has not been shown to be true in any studies outside of mailed survey studies, based on self-reporting by individual veterans. The subjects were uniformly older (59±7.2 years) white men, with one exception: a 38-year old African American man. Though this study is sufficient to reconfirm past findings and explore new imaging techniques in the GWI study at large, future studies drawing from the larger Gulf War

veteran population will establish a better baseline for broader analysis, and are already underway.

5.4 Conclusions

The main goal of this study was to investigate if T_2 relaxation values differ amongst the Haley-defined syndrome classifications of Gulf War Illness and veteran control subjects. The first aim of this study, to establish a technique that is both reproducible and sensitive to potential metabolite T_2 relaxation time changes in neurodegenerative diseases *in vivo*, was measurably accomplished in normal control subjects, and well-demonstrated in veteran control subjects, matched to ill veterans for age and education. This is a significant and new achievement, as T_2 values have previously been assumed to have little to no effect on metabolite concentration values, and reliable and reproducible protocols for measurement have not been previously established.

While significant differences in T_2 between some of the groups were observed, this difference alone was not found to be enough to differentiate between syndrome classifications in individual subjects.

This study represents an important extension of the previous brain metabolite MR spectroscopy study of Gulf War veterans, enabling the conclusion that, for short TE, reported significant changes in metabolite concentrations are due to actual biochemical

changes, not a false difference in signal intensity caused by significantly changed transverse relaxation times in illness.

This study provides a convincing argument to include T_2 relaxation measurements in future neurological spectroscopy studies, especially for those done with long TE times. The effect of T_2 correction is not negligible at long TE times, and the time needed to acquire a reliable and sensitive measurement is under 30 minutes per area of investigation.

6 FUTURE CONSIDERATIONS

6.1 Multi-Echo Water T_2 Decay Analysis

As the pilot study in GWI subjects progressed, an interesting observation was made within the MRS sub-core concerning the concentration values being obtained. The concentration ratios were not in good agreement with the quantitation of individual metabolites within subjects. This led to an investigation of the transverse relaxation time of water.

The water T_2 values, calculated from the logarithm of water peak values vs. echo time (TE) of the unsuppressed water acquisitions obtained for concentration calculation (TE=30/135/270 ms) varied significantly between syndrome classifications and veteran controls (mean difference 15.5%, p=0.02 between Syndrome 2 and veteran controls in left basal ganglia; mean difference 8%, p=0.04 between Syndrome 2 and veteran controls in right basal ganglia; mean difference 11.3%, p=0.004 between Syndrome 2 and Syndrome 3 in right basal ganglia; mean difference 10.2%, p=01 between Syndrome 2 and Syndrome 1 in right basal ganglia). Water T_2 data obtained in this study are shown in Figure 33. However, the regression fit is based on only three points, obtained with relatively few signal averages (4 averages for TE=30 ms, 8 for TE=135/270 ms), and had a high coefficient of variation (up to 18.8%).

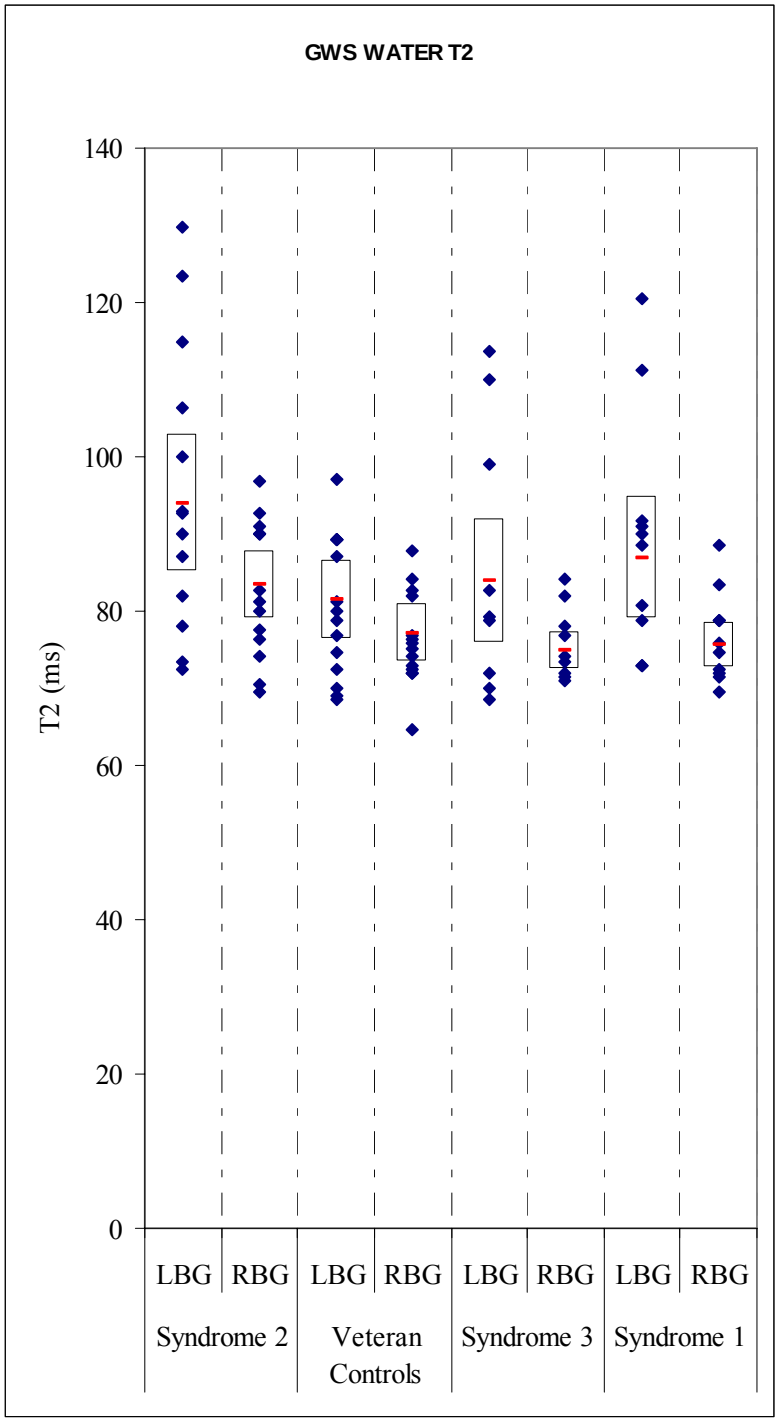

Figure 33. Water T_2 values measured in basal ganglia of Gulf War veterans. The box represents 2 standard deviations, ± 1 S.D from the mean (represented by horizontal dash).

Water T_2 not only has potential to differentiate between syndrome classifications of GWI, it may also have profound effect on concentration calculations. Absolute concentration calculations involve division by tissue water signal, which is in turn affected by water transverse relaxation. However, water also has potential to be affected by partial volume effects, creating a multi-exponential decay instead of a mono-exponential decay. If this is the case, the simple regression fit to three points will not be sufficient to characterize the true water transverse relaxation time(s).

The MRS sub-core, in particular Sandeep Kumar Ganji, interested in this new possibility, piloted methods proposed by Whittall and MacKay (Whittall, MacKay et al. 1997; Whittall, MacKay et al. 1999), and began investigating this aspect in the national survey phase of the GWI research project. Combined with segmentation of brain gray matter, white matter, and cerebrospinal fluid regions from high-resolution MP-RAGE anatomic images, this should produce more accurate water T_2 estimates for these three regions, minimally affected by partial volume averaging.

6.2 Ongoing GWI Study and Collaborations

As discussed earlier, the spectroscopy investigation is one avenue of exploration underway at the UT Southwestern Gulf War Illness Research Group. Many other studies are concurrent to the research presented here – other MRI imaging studies, EEG studies, psychiatric evaluations, autonomic and audiovestibular studies, and even animal studies. These other investigations, carried out by other members of the GWI Research Group at

large, will provide a fuller, more detailed picture of GWI and further inform our research in the MRS sub-core. In future correlation studies between various sub-cores, data from these different modalities will be combined and analyzed with the goal of defining a set of experiments and parameters which together have enough power and specificity to reliably identify GWI and distinguish amongst syndrome classifications on an individual subject basis, thus informing future research and treatment directions. Any additional theories on mechanisms of differing relaxation times in syndrome groups could also be elucidated by data from other research modalities.

APPENDIX A: RELAXATION MECHANISMS

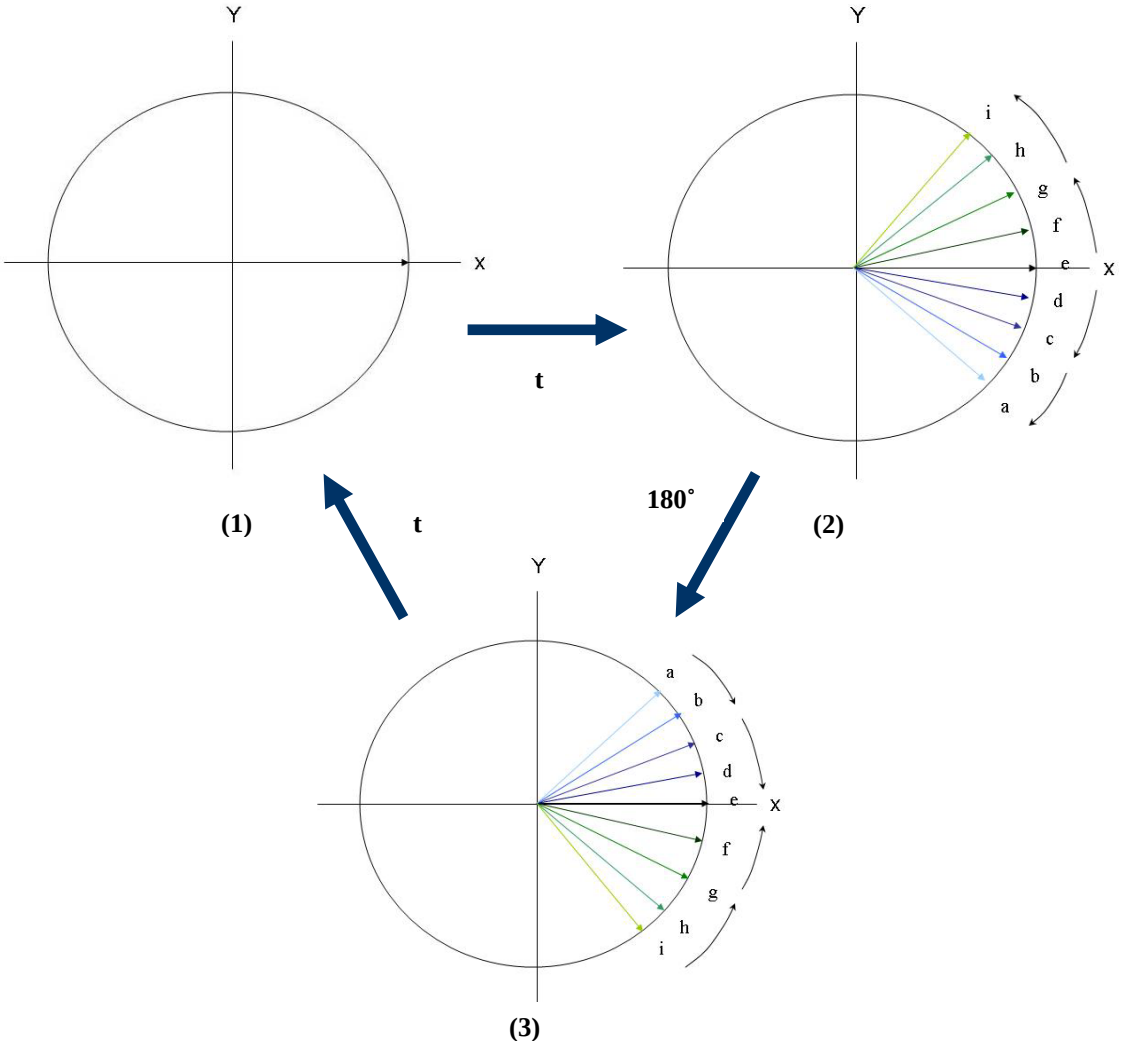

Figure 34. A diagram of a spin vectors in a spin-echo experiment, shown in a 2-dimensional rotating frame of reference. After a 90˚ pulse tilts the overall magnetization vector onto the x axis (1), the spins begin to dephase as they rotate over time t. As shown in (2), the spin labeled 'a' is precessing at a faster rate than other spins, and spin 'i' is precessing at a slower rate. After a 180˚ pulse is applied about the x axis, the position of spin vectors has been exchanged (3). Assuming the rate of the individual spins has not changed, after another elapsed time of t, the spins have rephased into the original vector shown in (1).

As shown in Figure 34, a typical sequence refocuses spins at time t=TE to create the echo signal. First, we investigate in more detail the transition during time t between (1) and (2) in this figure – what causes the loss of coherence in the precessing spins (ignoring the effects of longitudinal relaxation, previously discussed and minor effects calculated and incorporated into data analysis).

Any cause for fluctuations in magnetic fields at the site of the nucleus can be considered a relaxation mechanism. There are five established categories of relaxation interactions in chemical species in the field of NMR: dipole-dipole, quadrupole, chemical shift anisotropy, scalar (spin-spin coupling), and spin-rotation, each of which affects relaxation times via different interactions.

Scalar, or spin-spin coupling, refers to the indirect coupling of two nuclei via electrons, and potential changes in local field at the nucleus due to the relaxation of neighboring nuclei. A relaxation effect is created in spin I coupled to spin S in two cases: 1) The relaxation of S is very short compared to I, as is typically the case for quadrupolar spin $S > ½$ nuclei in asymmetric environments (see below), and 2) The coupling constant is time-dependent, as is the case when chemical exchange effects are present. Both of these cases would result in a fluctuating field which would in turn produce the scalar relaxation mechanism, however, this effect is typically very small compared to dipole-dipole interaction effects.

Chemical shift anisotropy refers to the effect the shielding vector σ, first shown in Equation 1-2 above, may have on shifting local fields at the nucleus if it has a directional dependence. This shielding effect for a hydrogen atom is small, but increases with

increasing atomic number. As for molecules, the presence of multiple nuclei hinders the potential rotation of electron clouds, thus creating a normally opposed force to the diamagnetic contribution, which is termed the paramagnetic shielding contribution.

The electric quadrupole moment relaxation mechanism refers to the charges surrounding the nucleus and any resulting electric field gradient experienced at the nucleus. The motion of an asymmetric charge distribution can create transitions in nuclear energy levels. This mechanism is often dominant for nuclei with spin $I > ½$, and is not relevant for proton spectroscopy, where spin $I = ½$.

The spin-rotation mechanism, conversely, refers to the motion of the molecular magnetic moment – the distribution of electrons over the entirety of the molecule. The effect of this mechanism is greater for small, symmetric, or gaseous molecules, which are more likely to have greater angular velocity. Furthermore, as temperature increases the spin rotation relaxation mechanism contributes more to relaxation, shortening T_1. This relationship between relaxation and temperature is opposite to the other mechanisms listed here. In the case of spin-rotation in this study, protons have been established to have a small range of chemical shifts, which also implies a distribution of electrons with small spin-rotation tensor component.

Dipole-dipole interactions is often the most important relaxation mechanism for spin ½ nuclei, and refers to the motion of nuclei in a molecule tumbling. It is the change in relative position in space of the neighboring nuclei, or unpaired electrons, which changes the field at the nucleus site and can induce relaxation.

As might be inferred from Figure 34, the transition from (3) to (1), where the spins refocus to create the signal, unless the spins are precessing at exactly the same rate during time t between (1) and (2) as they are during time t between (3) and (1), they will not all refocus into the original vector. Diffusion of molecules will cause them to experience different field strengths, $B_{0,}$ at different locations (assuming the field is not perfectly homogenous), resulting in a reduction of signal amplitude which increases with time t during which molecules could potentially diffuse. The amplitude of the echo as compared to the original spin vector is:

$$Amplitude \propto \exp[-(2t/T_2) - \frac{2}{3}\gamma^2 G^2 D^2 t^3] \qquad \text{(Equation B.1)}$$

Where D is the diffusion coefficient, t is the time elapsed (as shown in Figure 34), and G is the spatial magnetic field gradient (Becker 1980). For the effect of the pulse-field spoiling gradients, the equation becomes:

$$Amplitude \propto \exp[-(\Delta - \frac{\delta}{3})\delta^2 \gamma^2 g^2 D] \qquad \text{(Equation B.2)}$$

Where g is the gradient amplitude, with duration time δ, separated by displacement time Δ (Stejskal 1965; Callaghan 1991). The effect of diffusion in the presence of constant diffusion coefficient increases with increasing time and gradient strengths, and can contribute to error, as discussed in section 5.3, above.

Contributions to T_2 due to magnet inhomogeneities are typically considered separate from factors arising from molecular origins, and the resulting observed T_2 is defined as T_2^* as follows: $1/T_2^* = 1/T_{2\,(sample)} + 1/T_{2\,(inhomogeneities)}$

APPENDIX B: SIEMENS 3T PRESS SEQUENCE DETAILS

For this study the SVS PRESS sequence utilized the following parameters:

CHESS pulses: RF pulse duration 17.9ms, gradient amplitude 4.07 mT/m, gradient duration 41.3 ms

90-degree RF pulse: RF pulse duration 2.6ms, gradient amplitude 3.56 mT/m

180-degree RF pulse: RF pulse duration 5.2ms, spoiling gradient amplitude 7 mT/m, spoiling gradient duration 2ms, gradient amplitude 0.9 mT/m

180-degree RF pulse: RF pulse duration 5.2ms, spoiling gradient amplitude 11.5 mT/m, spoiling gradient duration 4 ms, gradient amplitude 1.35 mT/m

Ramp up and ramp down times for gradients were 0.8 ms. A rectangular reference pulse of 11.74 μT was used for calibration – the power is equal to the Hamming-filtered sinc pulse used for RF excitation and refocusing pulses. Water suppression bandwidth was 50 Hz, and data points = 1024.

In order to prevent directional bias from being introduced by inhomogeneity in the hardware, magnet systems often implement a phase cycle during repeated acquisitions. The phase cycle (EXOR-16) used by the current hardware is shown below, with phase units in degrees.

The rotations listed are applied to the excitation, phase direction refocusing, and slice direction refocusing pulses, as described in Figure 34, in order to remove directional bias. By using acquisitions numbered in multiples of 16 (N = 32, 64, 96 and 128 in the various acquisitions used, as discussed earlier), this error is not introduced into the data in this study.

Step 1,
excitation RF phase = 0;
phase direction refocus RF phase = 0;
slice direction refocus RF phase = 0;
readout direction refocus RF phase = 0;

Step 2,
excitation RF phase = 0;
phase direction refocus RF phase = 90;
slice direction refocus RF phase = 0;
readout direction refocus RF phase = 180;

Step 3,
excitation RF phase = 0;
phase direction refocus RF phase = 180;
slice direction refocus RF phase = 0;
readout direction refocus RF phase = 0;

Step 4,
excitation RF phase = 0;
phase direction refocus RF phase = 270;
slice direction refocus RF phase] = 0;
readout direction refocus RF phase = 180;

Step 5,
excitation RF phase = 0;
phase direction refocus RF phase = 0;
slice direction refocus RF phase = 90;
readout direction refocus RF phase = 180;

Step 6,
excitation RF phase = 0;
phase direction refocus RF phase = 90;
slice direction refocus RF phase = 90;
readout direction refocus RF phase = 0;

Step 7,
excitation RF phase = 0;
phase direction refocus RF phase = 180;
slice direction refocus RF phase = 90;
readout direction refocus RF phase = 180;

Step 8,
excitation RF phase = 0;
phase direction refocus RF phase = 270;
slice direction refocus RF phase = 90;
readout direction refocus RF phase = 0;

Step 9,
excitation RF phase = 0;
phase direction refocus RF phase = 0;
slice direction refocus RF phase = 180;
readout direction refocus RF phase = 0;

Step 10,
excitation RF phase = 0;
phase direction refocus RF phase = 90;
slice direction refocus RF phase = 180;
readout direction refocus RF phase = 180;

Step 11,
excitation RF phase = 0;
phase direction refocus RF phase = 180;
slice direction refocus RF phase = 180;
readout direction refocus RF phase = 0;

Step 12,
excitation RF phase = 0;
phase direction refocus RF phase = 270;
slice direction refocus RF phase = 180;
readout direction refocus RF phase = 180;

Step 13,
excitation RF phase = 0;
phase direction refocus RF phase = 0;
slice direction refocus RF phase = 270;
readout direction refocus RF phase = 180;

Step 14,
excitation RF phase = 0;
phase direction refocus RF phase = 90;
slice direction refocus RF phase = 270;
readout direction refocus RF phase = 0;

Step 15,
excitation RF phase = 0;
phase direction refocus RF phase = 180;
slice direction refocus RF phase = 270;
readout direction refocus RF phase = 180;

Step 16,
excitation RF phase = 0;
phase direction refocus RF phase = 270;
slice direction refocus RF phase = 270;
readout direction refocus RF phase = 0;

REFERENCES

Antonini, A., K. L. Leenders, et al. (1993). "T2 relaxation time in patients with Parkinson's disease." Neurology **43**(4): 697-700.

Barker, P. B., D. O. Hearshen, et al. (2001). "Single-voxel proton MRS of the human brain at 1.5T and 3.0T." Magn Reson Med **45**(5): 765-9.

Becker, E. D. (1980). High resolution NMR : theory and chemical applications. New York, Academic Press.

Bottomley, P. A. (1987). "Spatial localization in NMR spectroscopy in vivo." Ann N Y Acad Sci **508**: 333-48.

Brass, S. D., N. K. Chen, et al. (2006). "Magnetic resonance imaging of iron deposition in neurological disorders." Top Magn Reson Imaging **17**(1): 31-40.

Brief, E. E., K. P. Whittall, et al. (2005). "Proton T2 relaxation of cerebral metabolites of normal human brain over large TE range." NMR Biomed **18**(1): 14-8.

Cady, E. B. (1996). "Metabolite concentrations and relaxation in perinatal cerebral hypoxic-ischemic injury." Neurochem Res **21**(9): 1043-52.

Callaghan, P. T. (1991). Principles of nuclear magnetic resonance microscopy. Oxford [England] New York, Clarendon Press ; Oxford University Press.

Certaines, J. d., W. M. M. J. Bovée, et al. (1992). Magnetic resonance spectroscopy in biology and medicine : functional and pathological tissue characterization. Oxford ; New York, Pergamon Press.

Chaudhuri, A., B. R. Condon, et al. (2003). "Proton magnetic resonance spectroscopy of basal ganglia in chronic fatigue syndrome." Neuroreport **14**(2): 225-8.

Chen, J. C., P. A. Hardy, et al. (1993). "MR of human postmortem brain tissue: correlative study between T2 and assays of iron and ferritin in Parkinson and Huntington disease." AJNR Am J Neuroradiol **14**(2): 275-81.

Chen, J. G., H. C. Charles, et al. (2000). "Magnetic resonance spectroscopy in Alzheimer's disease: focus on N-acetylaspartate." Acta Neurol Scand Suppl **176**: 20-6.

Cheong, J. L., E. B. Cady, et al. (2006). "Proton MR spectroscopy in neonates with perinatal cerebral hypoxic-ischemic injury: metabolite peak-area ratios, relaxation times, and absolute concentrations." AJNR Am J Neuroradiol **27**(7): 1546-54.

Choe, B. Y., J. W. Park, et al. (1998). "Neuronal laterality in Parkinson's disease with unilateral symptom by in vivo 1H magnetic resonance spectroscopy." Invest Radiol **33**(8): 450-5.

Choi, C., N. J. Coupland, et al. (2006). "T2 measurement and quantification of glutamate in human brain in vivo." Magn Reson Med **56**(5): 971-7.

Choi, C., I. Dimitrov, et al. (2009). "In vivo detection of serine in the human brain by proton magnetic resonance spectroscopy ((1)H-MRS) at 7 Tesla." Magn Reson Med.

Christiansen, P., A. Schlosser, et al. (1995). "Reduced N-acetylaspartate content in the frontal part of the brain in patients with probable Alzheimer's disease." Magn Reson Imaging **13**(3): 457-62.

Clarke, C. E. and M. Lowry (2000). "Basal ganglia metabolite concentrations in idiopathic Parkinson's disease and multiple system atrophy measured by proton magnetic resonance spectroscopy." Eur J Neurol **7**(6): 661-5.

Drost, D. J., W. R. Riddle, et al. (2002). "Proton magnetic resonance spectroscopy in the brain: report of AAPM MR Task Group #9." Med Phys **29**(9): 2177-97.

Farrar, T. C. and E. D. Becker (1971). Pulse and Fourier transform NMR; introduction to theory and methods. New York,, Academic Press.

Fernando, J. C., B. Hoskins, et al. (1984). "Effect on striatal dopamine metabolism and differential motor behavioral tolerance following chronic cholinesterase inhibition with diisopropylfluorophosphate." Pharmacol Biochem Behav **20**(6): 951-7.

Ferraz-Filho, J. R., P. V. Santana-Netto, et al. (2009). "Application of magnetic resonance spectroscopy in the differentiation of high-grade brain neoplasm and inflammatory brain lesions." Arq Neuropsiquiatr **67**(2A): 250-3.

Fleysher, L., R. Fleysher, et al. (2007). "Optimizing the precision-per-unit-time of quantitative MR metrics: examples for T1, T2, and DTI." Magn Reson Med **57**(2): 380-7.

Frahm, J., H. Bruhn, et al. (1989). "Localized high-resolution proton NMR spectroscopy using stimulated echoes: initial applications to human brain in vivo." Magn Reson Med **9**(1): 79-93.

Frederick, B. D., I. K. Lyoo, et al. (2004). "In vivo proton magnetic resonance spectroscopy of the temporal lobe in Alzheimer's disease." Prog Neuropsychopharmacol Biol Psychiatry **28**(8): 1313-22.

Freed, V. H., R. Haque, et al. (1976). "Physicochemical properties of some organophosphates in relation to their chronic toxicity." Environ Health Perspect **13**: 77-81.

Freed, V. H., M. A. Matin, et al. (1976). "Role of striatal dopamine in delayed neurotoxic effects of organophosphorus compounds." Eur J Pharmacol **35**(1): 229-32.

Fukuda, K., R. Nisenbaum, et al. (1998). "Chronic multisymptom illness affecting Air Force veterans of the Gulf War." JAMA **280**(11): 981-8.

Gelman, N., J. M. Gorell, et al. (1999). "MR imaging of human brain at 3.0 T: preliminary report on transverse relaxation rates and relation to estimated iron content." Radiology **210**(3): 759-67.

Grahn, J. A., J. A. Parkinson, et al. (2008). "The role of the basal ganglia in learning and memory: Neuropsychological studies." Behav Brain Res.

Gray, H. and C. D. Clemente (1985). Anatomy of the human body. Philadelphia, Lea & Febiger.

Graybiel, A. M. (2000). "The basal ganglia." Curr Biol **10**(14): R509-11.

Haley, R. W. (2003). "Excess incidence of ALS in young Gulf War veterans." Neurology **61**(6): 750-6.

Haley, R. W., S. Billecke, et al. (1999). "Association of low PON1 type Q (type A) arylesterase activity with neurologic symptom complexes in Gulf War veterans." Toxicol Appl Pharmacol **157**(3): 227-33.

Haley, R. W., J. L. Fleckenstein, et al. (2000). "Effect of basal ganglia injury on central dopamine activity in Gulf War syndrome: correlation of proton magnetic resonance spectroscopy and plasma homovanillic acid levels." Arch Neurol **57**(9): 1280-5.

Haley, R. W., J. Hom, et al. (1997). "Evaluation of neurologic function in Gulf War veterans. A blinded case-control study." JAMA **277**(3): 223-30.

Haley, R. W. and T. L. Kurt (1997). "Self-reported exposure to neurotoxic chemical combinations in the Gulf War. A cross-sectional epidemiologic study." JAMA **277**(3): 231-7.

Haley, R. W., T. L. Kurt, et al. (1997). "Is there a Gulf War Syndrome? Searching for syndromes by factor analysis of symptoms." JAMA **277**(3): 215-22.

Haley, R. W., W. W. Marshall, et al. (2000). "Brain abnormalities in Gulf War syndrome: evaluation with 1H MR spectroscopy." Radiology **215**(3): 807-17.

Hall, W. A. and C. L. Truwit (2008). "Intraoperative MR-guided neurosurgery." J Magn Reson Imaging **27**(2): 368-75.

Hammen, T., A. Stadlbauer, et al. (2005). "Short TE single-voxel 1H-MR spectroscopy of hippocampal structures in healthy adults at 1.5 Tesla--how reproducible are the results?" NMR Biomed **18**(3): 195-201.

Harris, R. K. (1986). Nuclear magnetic resonance spectroscopy : a physicochemical view. Burnt Mill, Harlow, Essex, England

Somerset, NJ, USA, Longman Scientific & Technical ;

J. Wiley, Eastern Distribution Center [distributor].

Hom, J., R. W. Haley, et al. (1997). "Neuropsychological correlates of Gulf War syndrome." Arch Clin Neuropsychol **12**(6): 531-44.

Jamal, G. A. (1995). "Long term neurotoxic effects of chemical warfare organophosphate compounds (Sarin)." Adverse Drug React Toxicol Rev **14**(2): 83-4.

Kang, H. K., B. Li, et al. (2009). "Health of US veterans of 1991 Gulf War: a follow-up survey in 10 years." J Occup Environ Med **51**(4): 401-10.

Kato, T., H. Hamakawa, et al. (1996). "Choline-containing compounds detected by proton magnetic resonance spectroscopy in the basal ganglia in bipolar disorder." J Psychiatry Neurosci **21**(4): 248-54.

Kirov, II, L. Fleysher, et al. (2008). "Age dependence of regional proton metabolites T2 relaxation times in the human brain at 3 T." Magn Reson Med **60**(4): 790-5.

Klose, U. (1990). "In vivo proton spectroscopy in presence of eddy currents." Magn Reson Med **14**(1): 26-30.

Knoke, J. D. and G. C. Gray (1998). "Hospitalizations for unexplained illnesses among U.S. veterans of the Persian Gulf War." Emerg Infect Dis **4**(2): 211-9.

Kopell, B. H. and B. D. Greenberg (2008). "Anatomy and physiology of the basal ganglia: implications for DBS in psychiatry." Neurosci Biobehav Rev **32**(3): 408-22.

Kuznetsov, Y. E., Z. Caramanos, et al. (2003). "Proton magnetic resonance spectroscopic imaging can predict length of survival in patients with supratentorial gliomas." Neurosurgery **53**(3): 565-74; discussion 574-6.

Kwock, L., J. K. Smith, et al. (2006). "Clinical role of proton magnetic resonance spectroscopy in oncology: brain, breast, and prostate cancer." Lancet Oncol **7**(10): 859-68.

Li, B. S., J. S. Babb, et al. (2002). "Reproducibility of 3D proton spectroscopy in the human brain." Magn Reson Med **47**(3): 439-46.

Lin, M. S. (1984). "Measurement of spin-lattice relaxation times in double spin-echo imaging." Magn Reson Med **1**(3): 361-9.

Martin, W. R. (2007). "MR spectroscopy in neurodegenerative disease." Mol Imaging Biol **9**(4): 196-203.

McDonald, B. E., L. G. Costa, et al. (1988). "Spatial memory impairment and central muscarinic receptor loss following prolonged treatment with organophosphates." Toxicol Lett **40**(1): 47-56.

Menon, D. K., C. J. Baudouin, et al. (1990). "Proton MR spectroscopy and imaging of the brain in AIDS: evidence of neuronal loss in regions that appear normal with imaging." J Comput Assist Tomogr **14**(6): 882-5.

Menon, P. M., H. A. Nasrallah, et al. (2004). "Hippocampal dysfunction in Gulf War Syndrome. A proton MR spectroscopy study." Brain Res **1009**(1-2): 189-94.

Mitsumori, F., H. Watanabe, et al. (2009). "Estimation of brain iron concentration in vivo using a linear relationship between regional iron and apparent transverse relaxation rate of the tissue water at 4.7T." Magn Reson Med.

Mitsumori, F., H. Watanabe, et al. (2007). "Apparent transverse relaxation rate in human brain varies linearly with tissue iron concentration at 4.7 T." Magn Reson Med **58**(5): 1054-60.

Mlynarik, V., S. Gruber, et al. (2001). "Proton T (1) and T (2) relaxation times of human brain metabolites at 3 Tesla." NMR Biomed **14**(5): 325-31.

Montgomery, E. B., Jr. (2007). "Basal ganglia physiology and pathophysiology: a reappraisal." Parkinsonism Relat Disord **13**(8): 455-65.

Morey, L. C. (2007). Personality assessment inventory (PAI) : professional manual. Lutz, FL, Psychological Assessment Resources.

Narayana, P. A. (2005). "Magnetic resonance spectroscopy in the monitoring of multiple sclerosis." J Neuroimaging **15**(4 Suppl): 46S-57S.

Naressi, A., C. Couturier, et al. (2001). "Java-based graphical user interface for the MRUI quantitation package." MAGMA **12**(2-3): 141-52.

National Institutes of Health (U.S.). Office of the Director. (1994). The Persian Gulf experience and health : National Institutes of Health Technology Assessment Workshop Statement, April 27-29, 1994. [Bethesda, Md.?], National Institutes of Health, Office of the Director.

O'Neill, J., N. Schuff, et al. (2002). "Quantitative 1H magnetic resonance spectroscopy and MRI of Parkinson's disease." Mov Disord **17**(5): 917-27.

Petropoulos, H., S. D. Friedman, et al. (2006). "Gray matter abnormalities in autism spectrum disorder revealed by T2 relaxation." Neurology **67**(4): 632-6.

Pfisterer, W. K., W. P. Hendricks, et al. (2007). "Fluorescent in situ hybridization and ex vivo 1H magnetic resonance spectroscopic examinations of meningioma tumor tissue: is it possible to identify a clinically-aggressive subset of benign meningiomas?" Neurosurgery **61**(5): 1048-59; discussion 1060-1.

Preul, M. C., Z. Caramanos, et al. (1998). "Using pattern analysis of in vivo proton MRSI data to improve the diagnosis and surgical management of patients with brain tumors." NMR Biomed **11**(4-5): 192-200.

Provencher, S. W. (1993). "Estimation of metabolite concentrations from localized in vivo proton NMR spectra." Magn Reson Med **30**(6): 672-9.

Renshaw, P. F., B. Lafer, et al. (1997). "Basal ganglia choline levels in depression and response to fluoxetine treatment: an in vivo proton magnetic resonance spectroscopy study." Biol Psychiatry **41**(8): 837-43.

Richards, T. L. (1991). "Proton MR spectroscopy in multiple sclerosis: value in establishing diagnosis, monitoring progression, and evaluating therapy." AJR Am J Roentgenol **157**(5): 1073-8.

Roland, P. S., R. W. Haley, et al. (2000). "Vestibular dysfunction in Gulf War syndrome." Otolaryngol Head Neck Surg **122**(3): 319-29.

Ross, B., R. Kreis, et al. (1992). "Clinical tools for the 90s: magnetic resonance spectroscopy and metabolite imaging." Eur J Radiol **14**(2): 128-40.

Savage, E. P., T. J. Keefe, et al. (1988). "Chronic neurological sequelae of acute organophosphate pesticide poisoning." Arch Environ Health **43**(1): 38-45.

Schubert, F., F. Seifert, et al. (2002). "Serial 1H-MRS in relapsing-remitting multiple sclerosis: effects of interferon-beta therapy on absolute metabolite concentrations." MAGMA **14**(3): 213-22.

Smith, J. K., M. Castillo, et al. (2003). "MR spectroscopy of brain tumors." Magn Reson Imaging Clin N Am **11**(3): 415-29, v-vi.

Steele, L. (2000). "Prevalence and patterns of Gulf War illness in Kansas veterans: association of symptoms with characteristics of person, place, and time of military service." Am J Epidemiol **152**(10): 992-1002.

Stejskal, E. O. (1965). "Use of Spin Echoes in a Pulsed Magnetic-Field Gradient to Study Anisotropic, Restricted Diffusion and Flow." The Journal of Chemical Physics **43**: 3597-3603.

Traber, F., W. Block, et al. (2004). "1H metabolite relaxation times at 3.0 tesla: Measurements of T1 and T2 values in normal brain and determination of regional differences in transverse relaxation." J Magn Reson Imaging **19**(5): 537-45.

Tsai, S. Y., S. Posse, et al. (2007). "Fast mapping of the T2 relaxation time of cerebral metabolites using proton echo-planar spectroscopic imaging (PEPSI)." Magn Reson Med **57**(5): 859-65.

Tunc-Skarka, N., W. Weber-Fahr, et al. (2009). "MR spectroscopic evaluation of N-acetylaspartate's T2 relaxation time and concentration corroborates white matter abnormalities in schizophrenia." Neuroimage **48**(3): 525-31.

United States. Dept. of Veterans Affairs. Research Advisory Committee on Gulf War Veterans' Illnesses. (2008). Gulf War illness and the health of Gulf War veterans : scientific findings and recommendations. Washington, D.C., Research Advisory Committee on Gulf War Veterans' Illnesses.

Uysal, E., M. Erturk, et al. (2005). "Multivoxel magnetic resonance spectroscopy in gliomatosis cerebri." Acta Radiol **46**(6): 621-4.

Van Zijl, P. C. and P. B. Barker (1997). "Magnetic resonance spectroscopy and spectroscopic imaging for the study of brain metabolism." Ann N Y Acad Sci **820**: 75-96.

Waldman, A. D. and G. S. Rai (2003). "The relationship between cognitive impairment and in vivo metabolite ratios in patients with clinical Alzheimer's disease and vascular dementia: a proton magnetic resonance spectroscopy study." Neuroradiology **45**(8): 507-12.

Weiner, M. W., H. Hetherington, et al. (1989). "Clinical magnetic resonance spectroscopy of brain, heart, liver, kidney, and cancer. A quantitative approach." NMR Biomed **2**(5-6): 290-7.

Whittall, K. P., A. L. MacKay, et al. (1997). "In vivo measurement of T2 distributions and water contents in normal human brain." Magn Reson Med **37**(1): 34-43.

Whittall, K. P., A. L. MacKay, et al. (1999). "Are mono-exponential fits to a few echoes sufficient to determine T2 relaxation for in vivo human brain?" Magn Reson Med **41**(6): 1255-7.

Wilkinson, I. D., M. Paley, et al. (1994). "Proton spectroscopy in HIV infection: relaxation times of cerebral metabolites." Magn Reson Imaging **12**(6): 951-7.

Zaaraoui, W., L. Fleysher, et al. (2007). "Human brain-structure resolved T(2) relaxation times of proton metabolites at 3 Tesla." Magn Reson Med **57**(6): 983-9.

Zivadinov, R. and T. P. Leist (2005). "Clinical-magnetic resonance imaging correlations in multiple sclerosis." J Neuroimaging **15**(4 Suppl): 10S-21S.